Study to Establish Relations for the Relative Strength of API 650 Cone Roof Roof-to-Shell and Shell-to-Bottom Joints

API PUBLICATION 937-A
AUGUST 2005

API
American Petroleum Institute

Study to Establish Relations for the Relative Strength of API 650 Cone Roof Roof-to-Shell and Shell-to-Bottom Joints

API PUBLICATION 937-A
AUGUST 2005

Prepared by:
Thunderhead Engineering Consultants, Incorporated
1006 Poyntz Ave.
Manhattan, KS 66502-5459
785-770-8511
www.thunderheadeng.com

SPECIAL NOTES

API publications necessarily address problems of a general nature. With respect to particular circumstances, local, state, and federal laws and regulations should be reviewed.

Neither API nor any of API's employees, subcontractors, consultants, committees, or other assignees make any warranty or representation, either express or implied, with respect to the accuracy, completeness, or usefulness of the information contained herein, or assume any liability or responsibility for any use, or the results of such use, of any information or process disclosed in this publication. Neither API nor any of API's employees, subcontractors, consultants, or other assignees represent that use of this publication would not infringe upon privately owned rights.

API publications may be used by anyone desiring to do so. Every effort has been made by the Institute to assure the accuracy and reliability of the data contained in them; however, the Institute makes no representation, warranty, or guarantee in connection with this publication and hereby expressly disclaims any liability or responsibility for loss or damage resulting from its use or for the violation of any authorities having jurisdiction with which this publication may conflict.

API publications are published to facilitate the broad availability of proven, sound engineering and operating practices. These publications are not intended to obviate the need for applying sound engineering judgment regarding when and where these publications should be utilized. The formulation and publication of API publications is not intended in any way to inhibit anyone from using any other practices.

Any manufacturer marking equipment or materials in conformance with the marking requirements of an API standard is solely responsible for complying with all the applicable requirements of that standard. API does not represent, warrant, or guarantee that such products do in fact conform to the applicable API standard.

API FOREWORD

Nothing contained in any API publication is to be construed as granting any right, by implication or otherwise, for the manufacture, sale, or use of any method, apparatus, or product covered by letters patent. Neither should anything contained in the publication be construed as insuring anyone against liability for infringement of letters patent.

This document was produced under API standardization procedures that ensure appropriate notification and participation in the developmental process and is designated as an API standard. Questions concerning the interpretation of the content of this publication or comments and questions concerning the procedures under which this publication was developed should be directed in writing to the Director of Standards, American Petroleum Institute, 1220 L Street, N.W., Washington, D.C. 20005. Requests for permission to reproduce or translate all or any part of the material published herein should also be addressed to the director.

Generally, API standards are reviewed and revised, reaffirmed, or withdrawn at least every five years. A one-time extension of up to two years may be added to this review cycle. Status of the publication can be ascertained from the API Standards Department, telephone (202) 682-8000. A catalog of API publications and materials is published annually and updated quarterly by API, 1220 L Street, N.W., Washington, D.C. 20005.

Suggested revisions are invited and should be submitted to the Standards and Publications Department, API, 1220 L Street, NW, Washington, DC 20005, standards@api.org.

TABLE OF CONTENTS

1. Introduction

This report documents an evaluation of the relative strengths of the roof-to-shell and shell-to-bottom joints in API 650 cone roof tanks. This information is supplied to the American Petroleum Institute as background material for development of design rules that govern frangible roof joints for API 650 tanks.

API 650 (American Petroleum Institute, 2001) provides design criteria for fluid storage tanks used to store flammable products. Due to filling and emptying of the tanks, the vapor above the product surface inside the tank may be within its flammability limits. Ignition of this vapor can cause sudden over-pressurization and can lead to the catastrophic loss of tank integrity. To prevent shell or bottom failure, the rules in API 650 are intended to ensure that the frangible roof-to-shell joint fails before failure occurs in the tank shell or the shell-to-bottom joint. Failure of the frangible roof-to-shell joint provides a large venting area and reduces the pressure in the tank.

Although the criteria in API 650 function well for large tanks, small tanks designed to the API 650 rules have not always functioned as intended. Morgenegg, 1978, provides a description of a 20 foot diameter by 20 foot tall tank in which the shell-to-bottom failed. Other such failures have been noted by API, providing the incentive for this study.

As presently written, the API 650 rules do not address the strength of the shell-to-bottom joint directly. Instead, the present rule is intended to ensure that the roof-to-shell joint fails at a pressure lower than that required to lift the weight of tank. It is assumed that with no uplift, the shell-to-bottom joint will not have significant additional loads and that failure of the shell-to-bottom will be avoided.

A study of roof-to-shell joint failure (Swenson, et al., 1996) showed that for large tanks, the roof-to-shell joint did indeed fail before tank uplift, but that for smaller tanks uplift would occur before roof-to-shell joint failure. Since uplift occurs for small tanks, this increases the possibility of shell-to-bottom joint failure.

The purpose of this study is to investigate the relative strengths of the roof-to-shell and shell-to-bottom joints, with the goal of providing suggestions for frangible roof design criteria applicable to smaller tanks.

2. SafeRoof

The calculations in this report were made using the SafeRoof computer program (Lu and Swenson, 1994). SafeRoof was developed to design and analyze storage tanks with frangible roof joints. The program is the result of a research program into frangible joint design, sponsored by the American Petroleum Institute and the Pressure Vessel Research Council.

SafeRoof includes design, analysis, and post-processing modules. In the design module, the user can input tank parameters and SafeRoof will develop a design following API 650 guidelines. This design can either be accepted or modified. The user can then analyze the stresses and displacements in the tank at pressures corresponding to selected tank failure modes. The analysis can be coupled to a combustion/joint failure analysis. The pressures at each failure mode can be used to help evaluate safety of the tank due to overload pressures.

The original version of SafeRoof used a static, large displacement, elastic finite element model. As part of this project, version 2.0 was extended to incorporate the capability to perform dynamic, large displacement, elastic-plastic analyses of tank response. This capability is based on the FMA-3D code (FMA, 2004).

Version 2.1 includes the capability to approximate circumferential buckling in the roof and floor. Buckling is approximated by reducing the circumferential stiffness of the roof (or floor) finite elements by a factor of 10 in the elements in which compressive circumferential stresses are detected. Based on beam flange buckling practice, buckling effects are not included within a distance of 32 times the roof (or floor) thickness from the joint. In addition, for buckling of the floor, the floor must have uplifted from the supporting foundation.

3. Tank Response to Over-Pressurization

Before discussing the general results for the study, it is important to examine in detail the response of an oil storage tank to over-pressurization, based on previous work (Swenson et al., 1996). A tank with a 30 foot diameter and a 32 foot height will be discussed as a representative tank. The tank parameters are given in Figure 3-1.

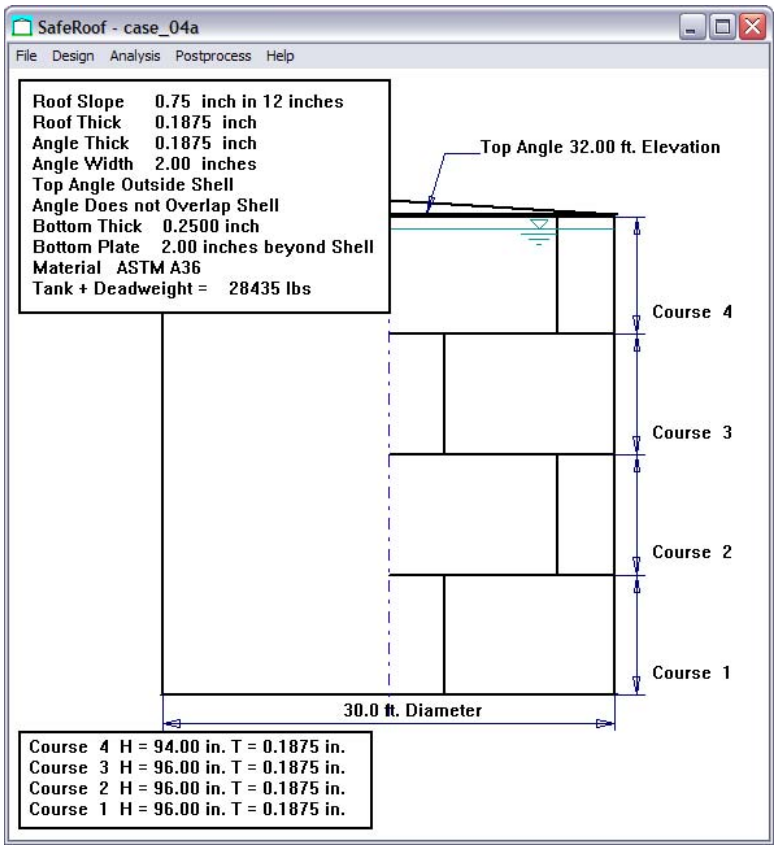

Figure 3-1: Design of representative 30 foot diameter tank

This design was done using the SafeRoof program (Lu and Swenson, 1994). This program follows API 650 rules to design the tank. The maximum fluid level is assumed to be 31 feet, with a specific gravity of 0.95. The material is ASTM A36, with a minimum yield strength of 36,000 psi, a modulus of 30E6 psi, and a Poisson's ratio of 0.25. In this example, the minimum yield strength was used, however, the typical yield strength should be used for design calculations.

The design has four courses with a thickness of 0.1875 inch. The top angle faces radially outward, with an angle width of 2 inches and a thickness of 0.1875 inches. The roof is welded to the top angle at a distance of 1 inch outside the radius of the tank. The slope of the roof is 0.75 inches in 12 inches. The bottom thickness is 0.25 inches. The tank is assumed to rest on sand, with a ringwall foundation. The stiffness of the sand is assumed to be 250 lb/sq. in/in and the stiffness of the foundation is assumed to be 1,000 lb/sq. in/in. The inner radius of the ringwall is

14.5 ft. The weight of the roof and tank shell is calculated to be 28,400 lbs. This does not include any deadweight due to stairways or other attachments.

As will be discussed, the roof-to-shell and shell-to-bottom joints act in circumferential compression at their respective failure pressures. This can lead to circumferential buckling of the roof near the roof-to-shell joint. The same buckling can occur at the shell-to-bottom joint, although to a lesser extent. If buckling occurs, it reduces the participation of the roof in carrying the compressive load at the joint. This leads to a lower calculated failure pressure than if buckling is not taken into account. This will be discussed for the case of an empty tank.

3.1 Empty Tank (no buckling)

We will first examine the response of the empty tank to four cases:

- Zero internal gauge pressure
- The pressure required to just cause uplift of the tank
- The pressure at failure of the roof-to-shell joint
- The pressure at failure of the shell-to-bottom joint

These results are based on the elastic, large deformation, static finite element analysis in SafeRoof. Results for inelastic, large deformation, dynamic analyses are similar and are presented later in this report.

3.1.1 Zero Internal Gauge Pressure

At zero internal gauge pressure and for an empty tank, the only load is the weight of the tank. As shown in Figure 3-2, there is little displacement except at the foundation. Figure 3-3 shows a detail of this displacement, which has a value of -0.005 inch directly under the tank shell. A plot of the equivalent stress (which can be used to predict onset of yielding), is shown in Figure 3-4. The stress is largest slightly above the shell-to-bottom, however the maximum stress is only 280 psi, so it is very low.

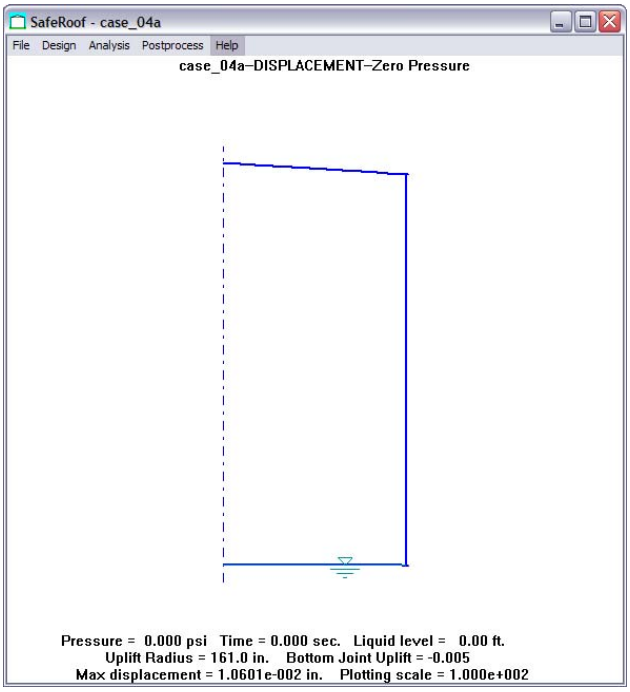

Figure 3-2: Tank displacement at zero internal gauge pressure (magnification=100x)

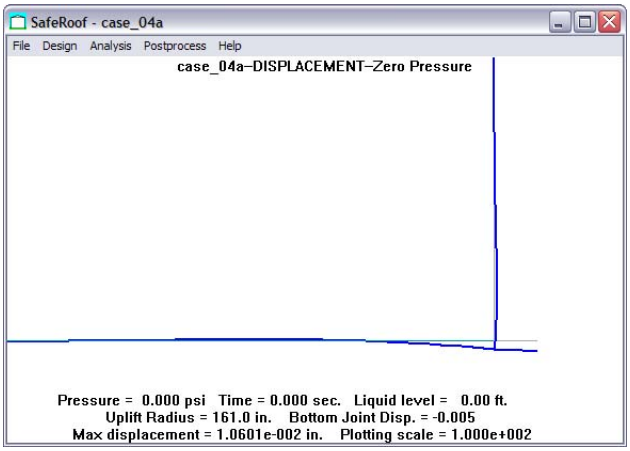

Figure 3-3: Detail of displacement of empty tank at foundation (magnification=100x)

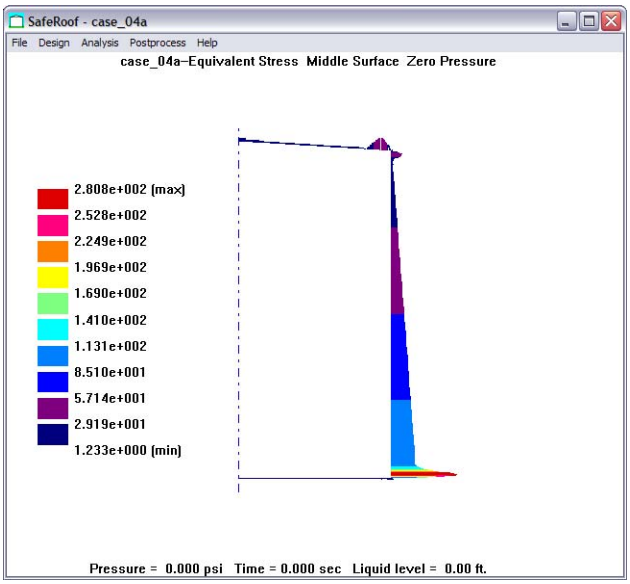

Figure 3-4: Middle surface equivalent stress contours in empty tank (min=0 psi, max=280 psi)

3.1.2 Balanced Uplift Pressure

Using the SafeRoof program, the pressure needed to just cause uplift of the empty tank (the "balanced uplift pressure" is calculated to be 0.295 psi. The deformed tank shape at this pressure is shown in Figure 3-5. The roof has lifted off the rafters and the displacement at the bottom of the shell is zero. The equivalent stresses shown in Figure 3-6 show that the peak stress is now at the roof-to-shell joint. However, the maximum equivalent stress is 10,370 psi, still below the yield stress of 36,000 psi. Therefore, no failure has occurred in the tank.

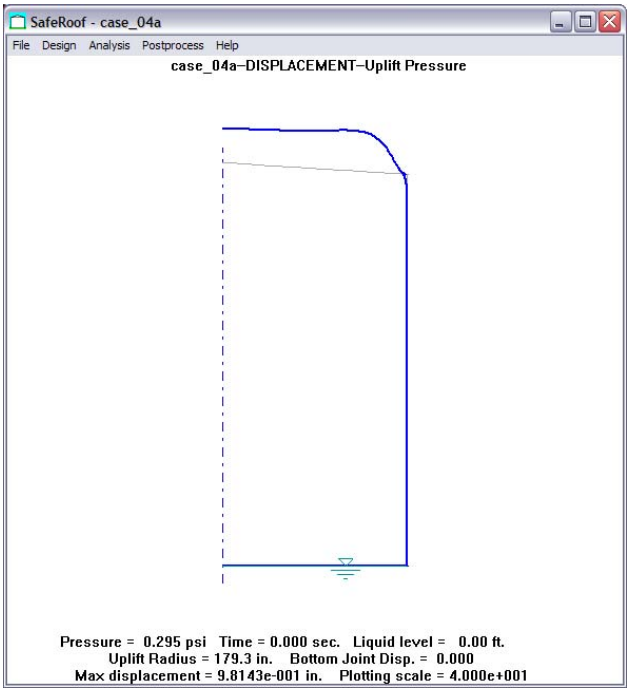

Figure 3-5: Displacement of empty tank at balanced uplift pressure (magnification=40x)

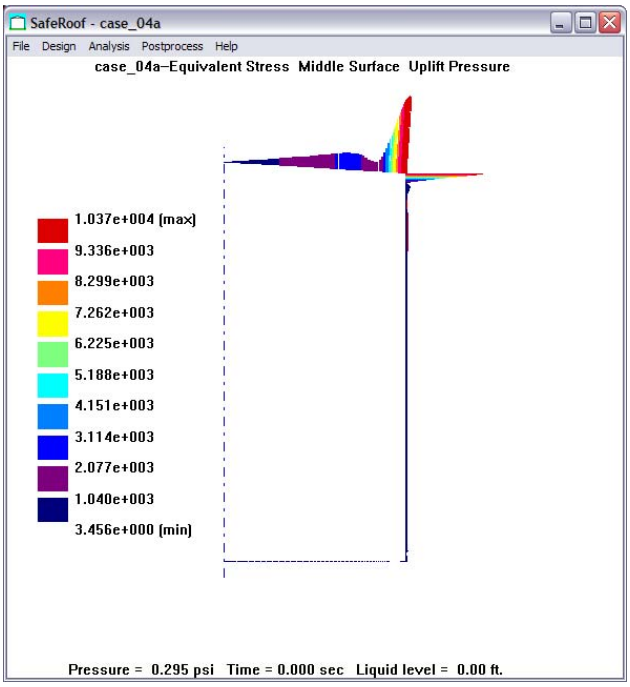

Figure 3-6: Middle surface equivalent stress at balanced uplift pressure (min=0 psi, max=10,370 psi)

3.1.3 Roof-to-Shell Joint Failure Pressure

Using the SafeRoof program, the pressure for failure of the roof-to-shell joint was calculated to be 1.04 psi. The criterion for failure of the roof-to-shell is yielding at the roof-to-shell joint in compression. This yielding then results in local buckling and kinking of the angle which causes the roof attachment weld to fail and to initiate detachment of the roof. Since the roof-to-shell failure pressure is greater than the balanced uplift pressure of 0.295 psi, significant uplift occurs before the roof-to-shell fails.

Both the roof-to-shell and the shell-to-bottom joints are in compression, as shown in the details of Figure 3-8 and Figure 3-9. This is due to the "doming" that has occurred in the roof (where it has lifted from the rafters) and the "bowling" of the tank bottom (which has resulted in a concave bottom). The deformations of both the roof and bottom result in inward radial displacements at the roof-to-shell and shell-to-bottom joints and a corresponding compressive circumferential stress.

At the bottom, the radius at which uplift starts is 98 inches (8.16 feet), so that the bottom has uplifted for a radial distance of 6.83 feet from the tank wall. The uplift displacement of the tank shell is 4.6 inches.

Equivalent stresses for the middle surface are plotted in Figure 3-10. These show that the top angle is at yielding (approximately 36,000 psi), while the stresses at the shell-to-bottom joint are large (approximately 26,000 psi), but not yet at yielding. At this load, the circumferential stresses in the bottom near the shell are in compression, Figure 3-11. The meridional stresses are in tension, with the largest (approximately 5,300 psi) values in the center of the bottom. However, in all cases, the meridional tension stresses in the bottom are much smaller than the circumferential stresses near the shell-to-bottom joint. Therefore, they are not expected to cause failure.

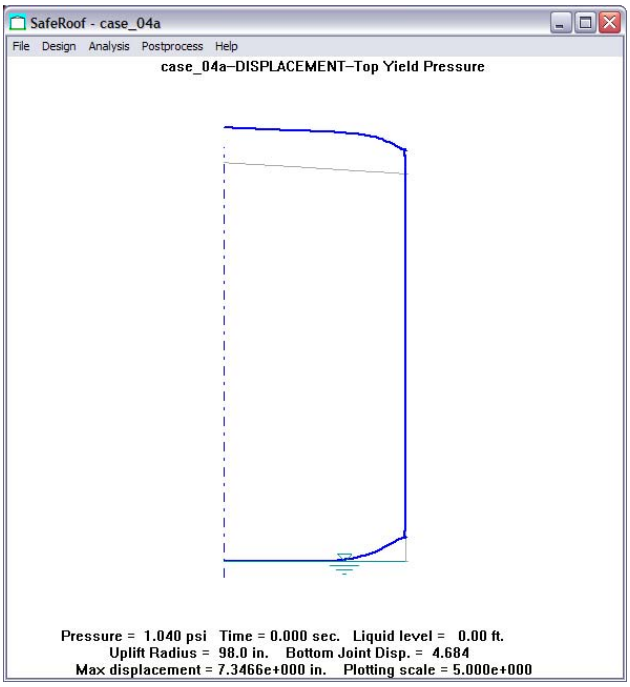

Figure 3-7: Displacement at roof-to-shell joint failure pressure (magnification=5x)

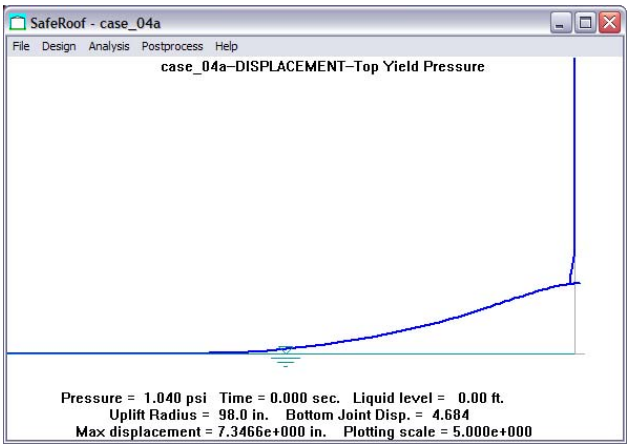

Figure 3-8: Detail of bottom displacement at roof-to-shell joint failure pressure (magnification=5x)

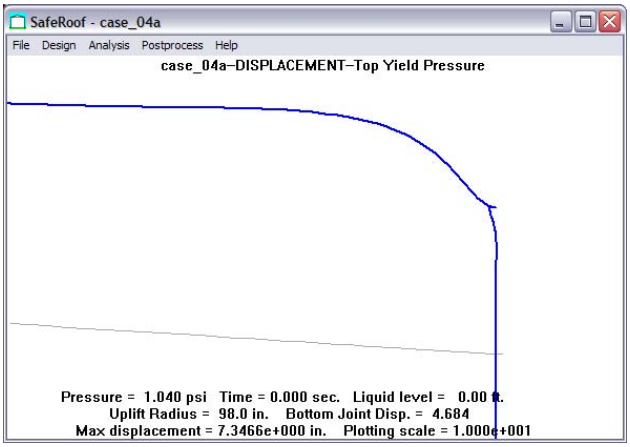

Figure 3-9: Detail of top displacement at roof-to-shell joint failure pressure (magnification = 10x)

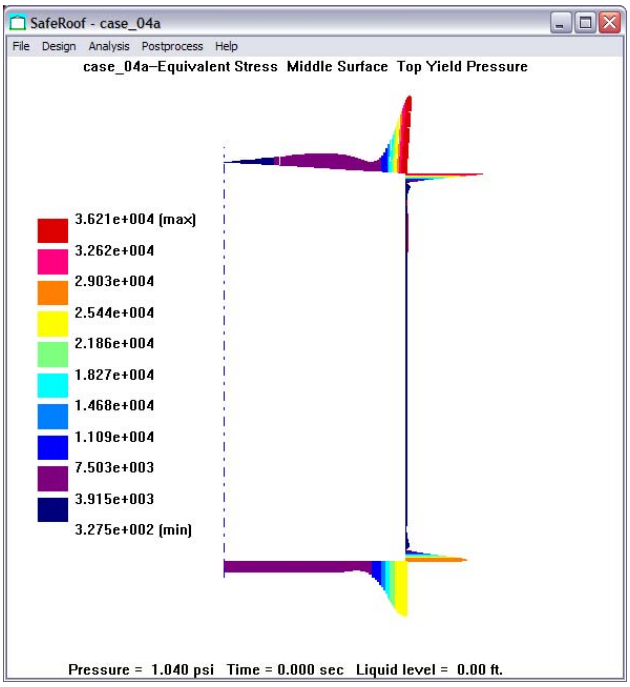

Figure 3-10: Middle surface equivalent stress at roof-to-shell joint failure pressure (min=330 psi, max=36,210 psi)

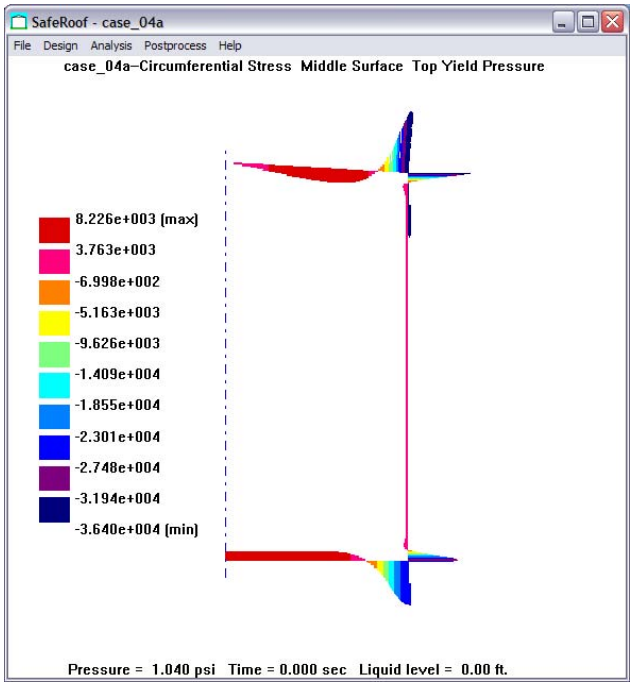

Figure 3-11: Middle surface circumferential stress at roof-to-shell joint failure pressure (min=-36,400 psi, max=8,230 psi)

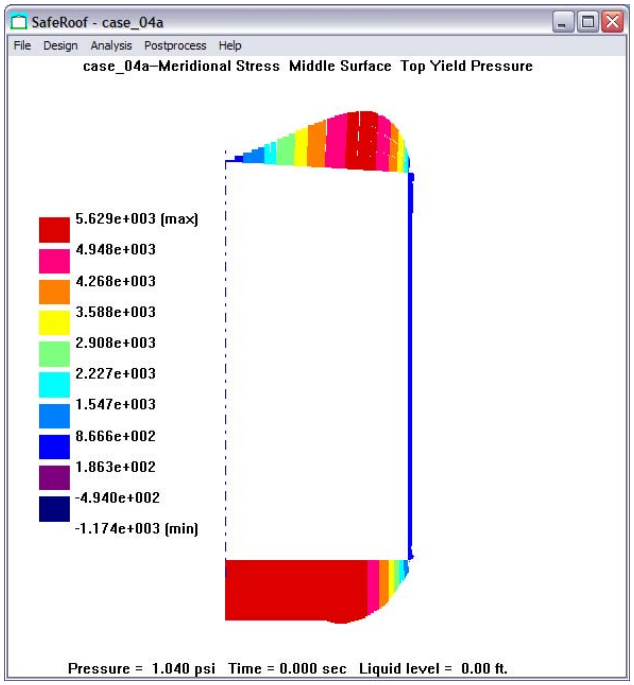

Figure 3-12: Middle surface meridional stress at roof-to-shell joint failure pressure (min=-11,740, max=5,630 psi)

3.1.4 Shell-to-Bottom Joint Failure Pressure

The calculated shell-to-bottom joint failure pressure is 1.27 psi for the empty tank. Bottom failure pressure is defined to be the pressure at which the shell-to-bottom joint reaches yielding. The largest stress component is the circumferential compressive stress that results from the "bowling" of the bottom as the shell uplifts. This "bowling" draws the outer radius of the bottom (and of the bottom of the shell) radially inward, causing the large compressive stress. As for the roof-to-shell joint, the failure mode is local buckling at the shell-to-bottom joint.

The tank deformed at this pressure is shown in Figure 3-13. At this higher pressure, the uplift radius is reduced to 90 inches and the magnitude of the uplift is increased to 5.5 inches.

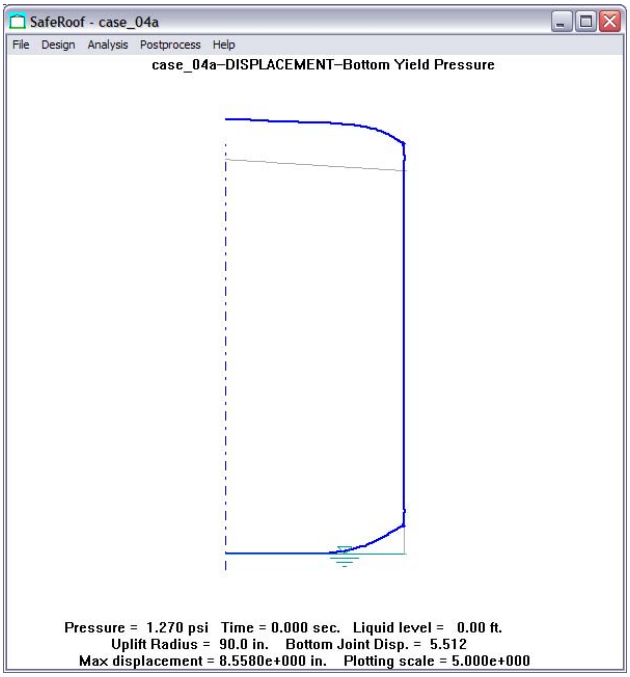

Figure 3-13: Deformation at shell-to-bottom joint failure pressure (magnification=5x)

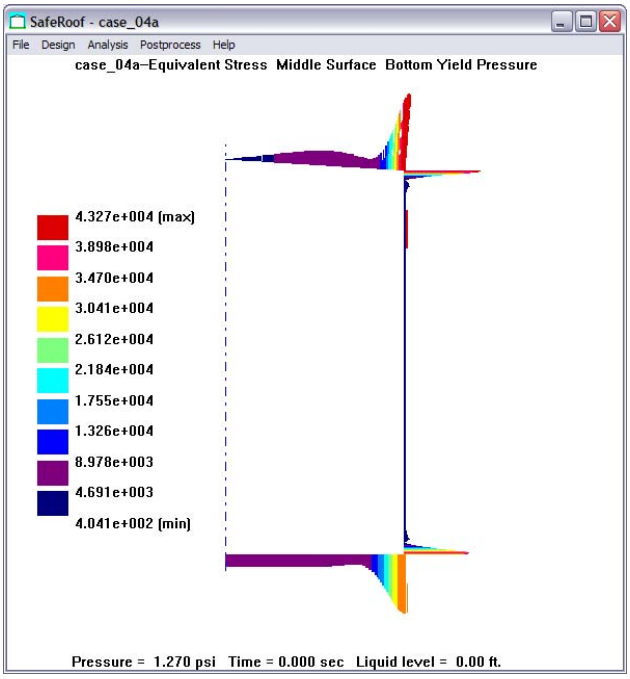

Figure 3-14: Middle surface equivalent stresses at shell-to-bottom joint failure pressure (min=400 psi, max=43,270 psi)

3.2 Full Tank (no buckling)

The response of a full tank is different at the shell-to-bottom joint. Because the product level does not affect the roof-to-shell joint, the failure pressure of the roof-to-shell joint will remain the same for both empty and full tanks. As for the empty tank, we will examine the response of the full tank to four cases:

- Zero internal gauge pressure
- The pressure required to just cause uplift of the tank
- The pressure at failure of the roof-to-shell joint
- The pressure at failure of the shell-to-bottom joint

These results are based on the elastic, large deformation, static finite element analysis in SafeRoof. Results for inelastic, large deformation, dynamic analyses are similar and are presented later in this report.

3.2.1 Zero Internal Gauge Pressure

The displacements for a full tank at zero internal gauge pressure are shown in Figure 3-15 and Figure 3-16. Figure 3-16 clearly shows the downward displacement of the bottom due to the pressure load of the product. The product also causes the circumferential stress to increase approximately linearly with depth, Figure 3-17. However, at the shell-to-bottom joint, the bottom (which is relatively stiff in tension) constrains the radial displacement of the shell, decreasing the circumferential stresses near the joint.

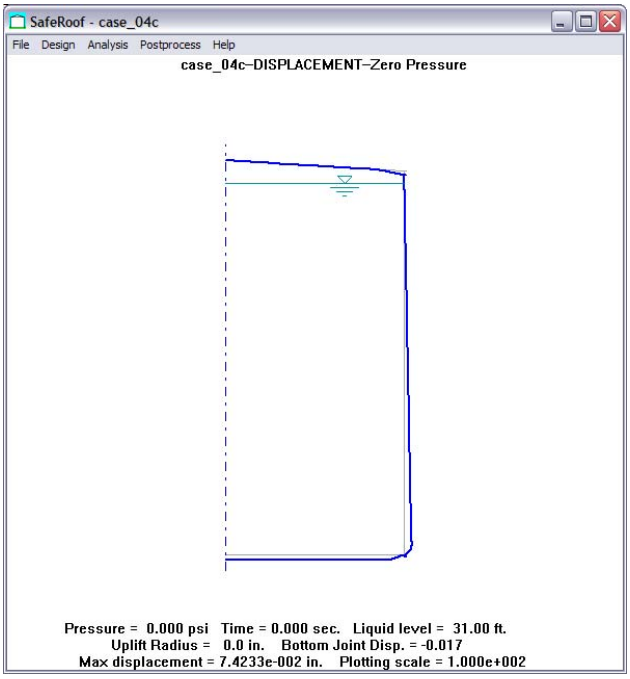

Figure 3-15: Displacement for a full tank at zero internal gauge pressure (magnification=100x)

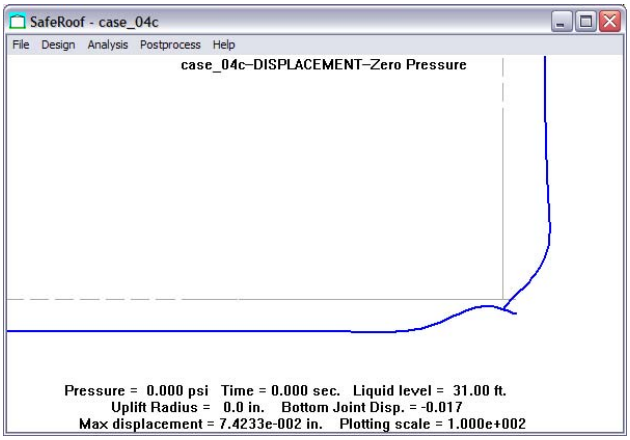

Figure 3-16: Detail of displacement for full tank at zero internal gauge pressure (magnification=100x)

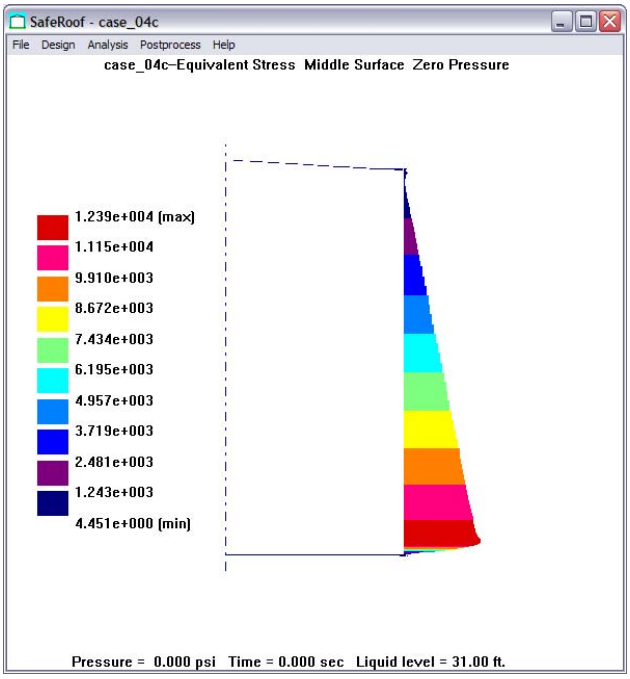

Figure 3-17: Middle surface equivalent stress for a full tank at zero internal gauge pressure (min=0 psi, max=12,390 psi)

3.2.2 Balanced Uplift Pressure

The full tank balanced uplift pressure is calculated to be 0.80 psi. A full tank has a higher balanced uplift pressure because the tank is resting on an elastic foundation. The force to uplift the tank must not only be greater than the tank weight, but it must also be sufficient to compensate for the reduced support of the elastic foundation as the bottom is lifted, Figure 3-18.

Even though the balanced uplift pressure for a full tank is greater than for an empty tank, the balanced uplift pressure is still smaller than the failure pressure of the roof-to-shell joint, so some uplift will occur before the frangible joint fails and relieves the internal pressure.

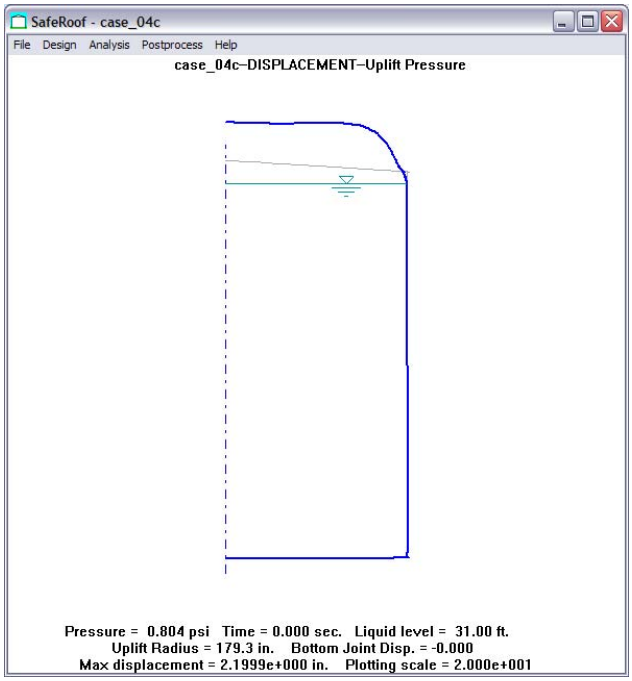

Figure 3-18: Displacement of full tank at balanced uplift pressure (magnification=20x)

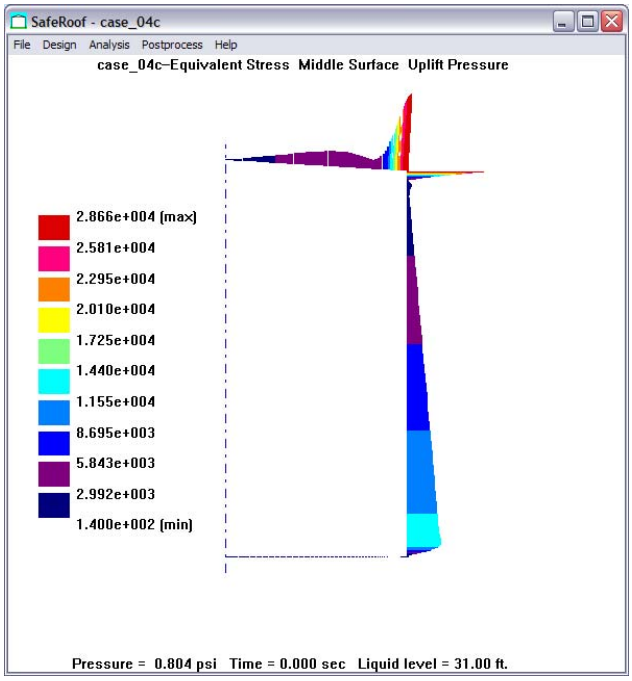

Figure 3-19: Middle surface equivalent stress at balanced uplift pressure (min=140 psi, max=28,660 psi)

3.2.3 Roof-to-Shell Joint Failure Pressure

The failure pressure of the roof-to-shell joint remains the same as the empty tank (1.04 psi), however the displacements at the shell-to-bottom joint are very different than for the empty case, Figure 3-20 and Figure 3-21. Although there is some uplift, the radius of first uplift is 176 inches (14.6 feet), nearly equal to the tank radius of 15 feet. The magnitude of the bottom uplift is also much smaller, at 0.027 inch.

Because the uplift is less, the stresses at the shell-to-bottom joint for a full tank at the roof-to-shell joint failure pressure are also less than an empty tank. For the empty tank the stress was approximately 26,000 psi, while for the full tank the shell-to-bottom joint stress is approximately 13,000 psi. Thus, a tank full of product has the effect of actually reducing the stress at the shell-to-bottom joint at the roof-to-shell joint failure pressure.

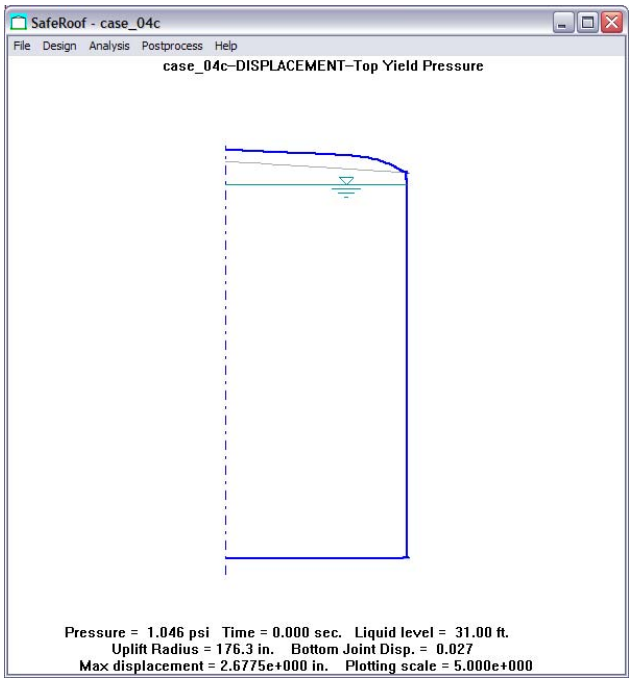

Figure 3-20: Displacement of full tank at roof-to-shell failure pressure (magnification=5x)

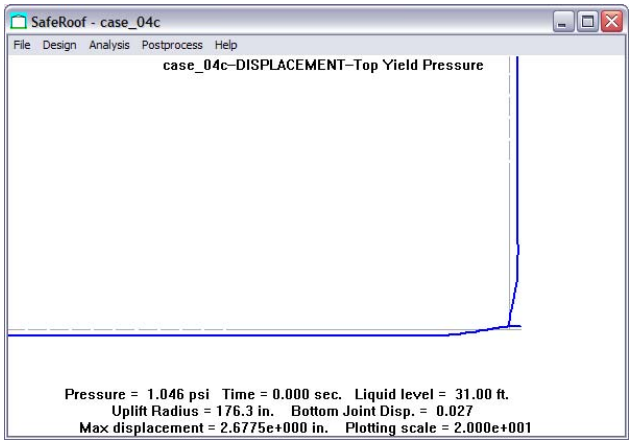

Figure 3-21: Detail of displacement for full tank at top failure pressure (magnification=20x)

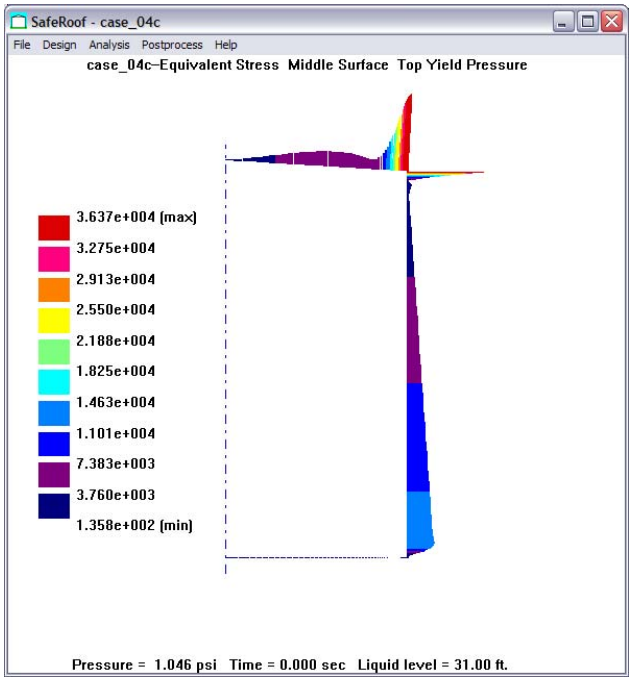

Figure 3-22: Middle surface equivalent stress at roof-to-shell joint failure pressure (min=130 psi, max=36,370 psi)

3.2.4 Shell-to-Bottom Joint Failure Pressure

The shell-to-bottom joint failure pressure for a full tank is calculated to be 3.25 psi. The displacements at this pressure are shown in Figure 3-23 and Figure 3-24. At this pressure the radius of first uplift is 161 inches (13.4 feet). The uplift magnitude is 2.35 inches.

Stresses are plotted in Figure 3-25. At this pressure, the stresses in the shell-to-bottom are just at yielding (the elastic roof-to-shell joint stresses have far exceeded yielding).

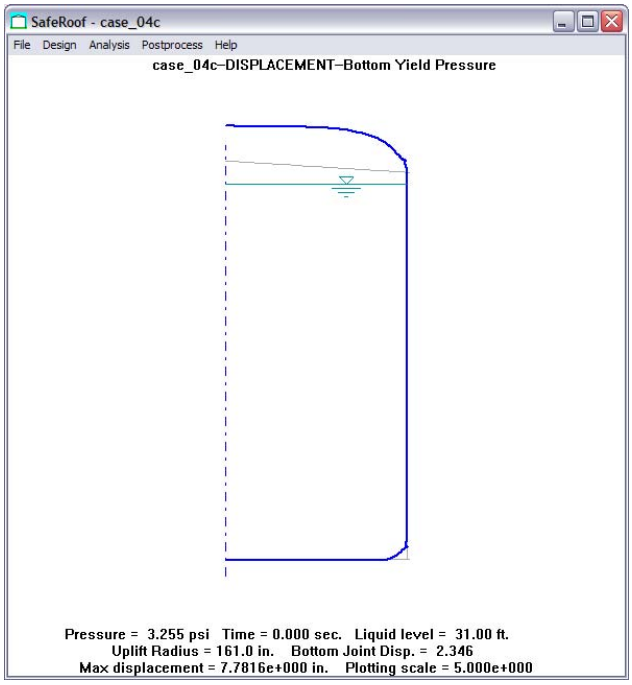

Figure 3-23: Displacement of full tank (magnification=5x)

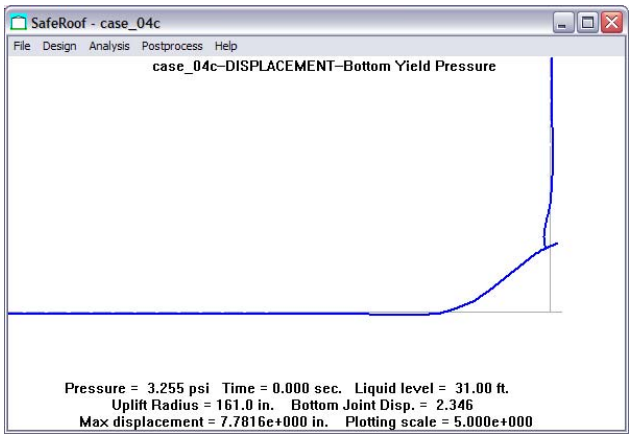

Figure 3-24: Detail of displacement for full tank (magnification=5x)

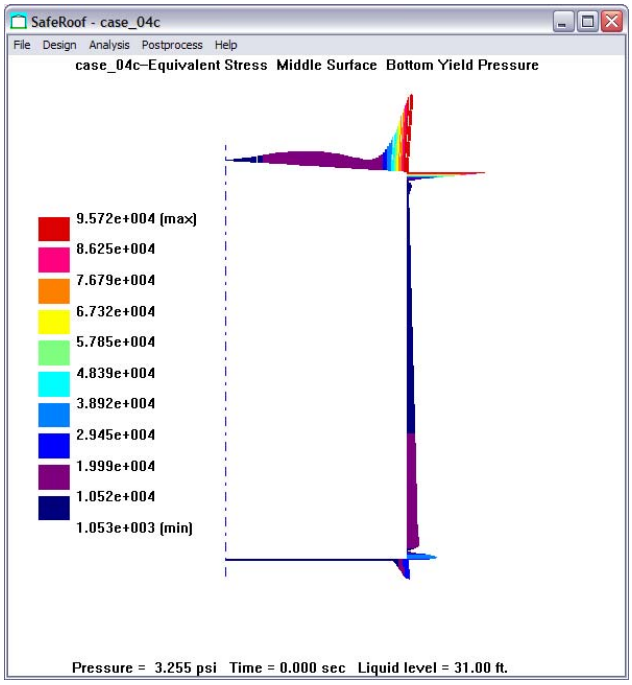

Figure 3-25: Middle surface equivalent stress at shell-to-bottom joint failure pressure (min=1,050 psi, max=95, 720 psi)

3.3 Empty Tank (with buckling)

As noted, buckling can reduce the strength of the joints. We will examine in detail the effect of buckling on the pressure at failure of the roof-to-shell joint. Buckling is approximated in the elastic, large deformation, static finite element analyses by reducing the compressive strength of roof and floor when compressive stresses are detected.

3.3.1 Roof-to-Shell Joint Failure Pressure

Buckling is approximated in the SafeRoof analysis by reducing the circumferential stiffness of the elements in compression in the roof or floor. Based on beam flange buckling practice, buckling effects are not included within a distance of 32 times the roof (or floor) thickness from the joint.

When buckling is included, the pressure for failure of the roof-to-shell joint was calculated to be 0.724 psi as compared to 1.04 psi without buckling. These two values give a range at which the actual failure would be expected. Since both of these roof-to-shell failure pressures are greater than the balanced uplift pressure of 0.295 psi, significant uplift occurs before the roof-to-shell fails, as shown in Figure 3-26.

Equivalent stresses for the middle surface are plotted in Figure 3-27. Comparing these results to those without buckling (Figure 3-10) shows that buckling has significantly reduced the participation of the roof in resisting the circumferential compressive load. The load is being carried by the angle and the short section of the roof near the joint. The circumferential and meridional stresses are shown in Figure 3-28 and Figure 3-29.

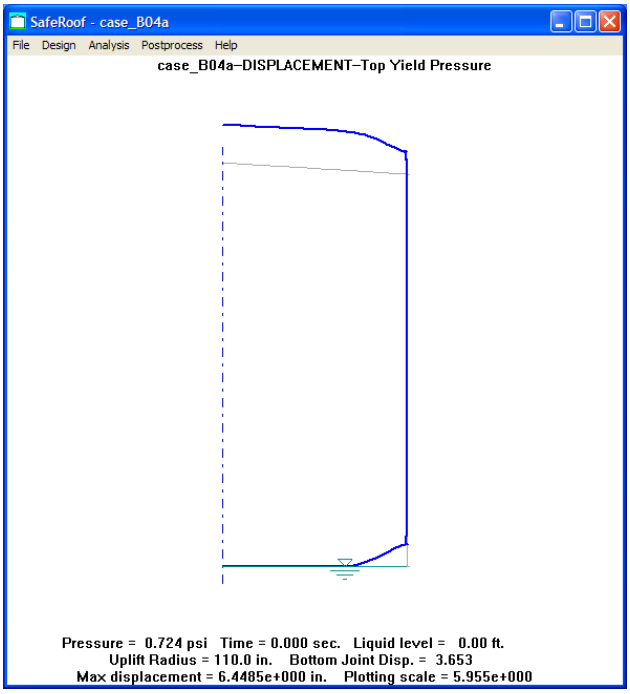

Figure 3-26: Displacement at roof-to-shell joint failure pressure

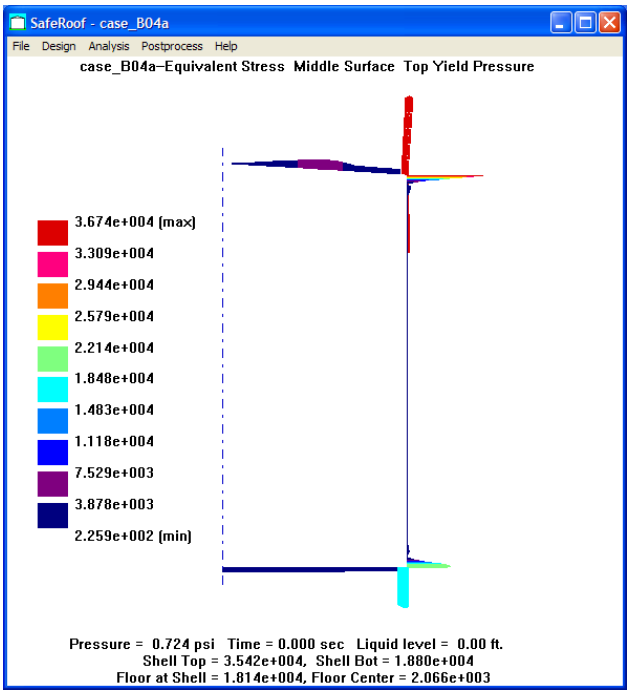

Figure 3-27: Middle surface equivalent stress at roof-to-shell joint failure pressure (min=225 psi, max=36,740 psi)

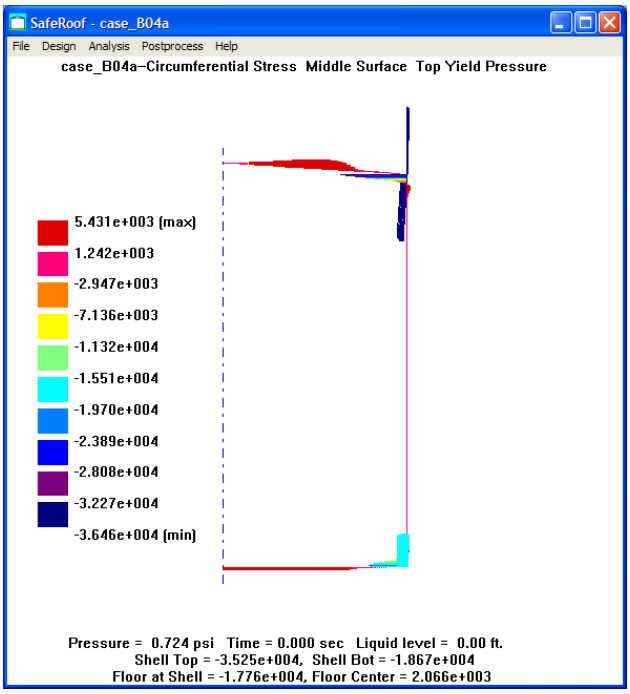

Figure 3-28: Middle surface circumferential stress at roof-to-shell joint failure pressure (min=-36,460 psi, max=5,430 psi)

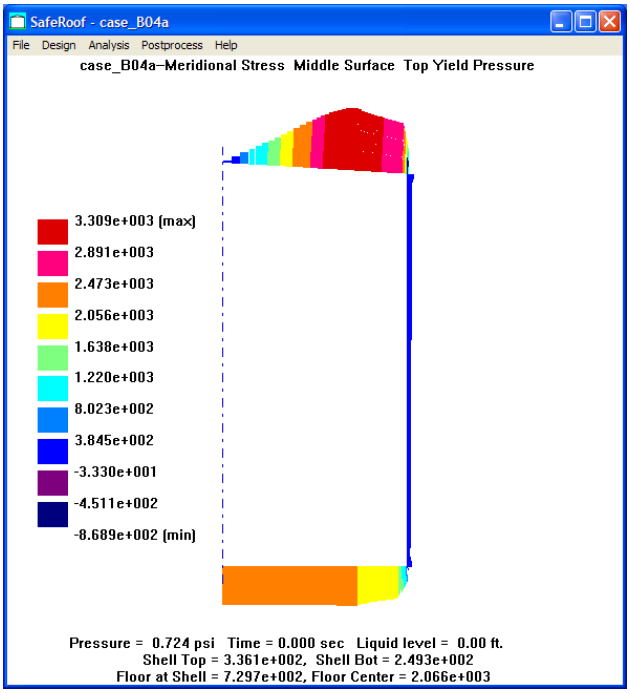

Figure 3-29: Middle surface meridional stress at roof-to-shell joint failure pressure (min=-870, max=3,310 psi)

3.4 Summary of Responses

The results presented above highlight the primary features of tank response:

1. Balanced uplift pressures are a function of product level. Empty tanks uplift at a lower pressure than full tanks, for this 30x32 foot tank the uplift pressures are 0.295 psi empty and 0.804 full.
2. The effect of buckling in the roof (and floor) can be significant. Without buckling, the roof-to-shell joint is predicted to fail at 1.04 psi, with buckling the predicted failure pressure is 0.724 psi. It is expected that the actual failure pressure lies between these two bounds.
3. Significant uplift can occur at the pressure required to fail the roof-to-shell joint, for this tank the uplift was 4.64 inches (no buckling) and 3.65 inches (with buckling) when empty and negligible when full. This uplift could cause attachments to fail. It could also lead to loads on the bottom that could cause failure.
4. The difference between the pressure to cause failure of the roof-to-shell joint and the shell-to-bottom joint is relatively small for empty tanks. In this case, the pressure to cause failure of the roof-to-shell joint when empty was 1.04 psi and 1.27 psi for failure of the shell-to-bottom joint (0.72 psi and 1.06 psi respectively with buckling). When full, the pressures were 1.04 psi for the roof-to-shell joint and 3.26 psi for the shell-to-bottom joint (0.72 psi and 3.24 psi respectively with buckling). Thus, the joint failure ratio (ratio of bottom joint failure to top joint failure) for empty small tanks can be low. For full tanks, the joint failure ratio is larger.

This behavior must be considered when developing new design criteria. Since uplift may not be prevented, the new criteria must accommodate uplift. This introduces several new failure modes: shell-to-bottom joint yield, weld failure of the shell-to-bottom joint, and failure of the bottom lap joints. These are addressed in the new suggested design criteria.

4. Failure Modes

In this section, we discuss the potential failure modes appropriate for the case where significant uplift will occur as part of tank over-pressurization. Protecting against these new failure modes will require an extension of the present API 650 rules, which assume no uplift. The possibility of uplift makes it necessary to examine the strength of the shell-to-bottom in more detail and to look at failure modes in the bottom.

In discussing failure modes, it is important to recognize that yielding is not necessarily a failure condition, it depends on the type of yielding that is occurring. If "primary" stresses in a structure cause yielding, then failure does occur. "Primary" stresses are stresses that are necessary to maintain equilibrium. However, yielding due to bending or local stress concentrations may not cause failure.

For example, in a tank at the roof-to-shell joint there can be high bending moments and radial shear loads that cause yielding at the inner or outer surface of the shell. If as the average stress in the shell remains below yielding this will not result in gross failure, since the shell will just increase curvature. However, if the average stress through the thickness of the shell exceeds the yield stress, failure will result, since the structure is no longer be able to resist the applied loads and gross deformations will result.

4.1 Roof-to-Shell Joint Failure

Failure of the roof-to-shell is due to yielding at the top angle in compression, followed by local buckling and kinking which causes the weld attaching the roof to the angle to fail, relieving pressure in the tank. This failure mode is supported both by testing (Swenson et al., 1996) and by field observations, Figure 4-1.

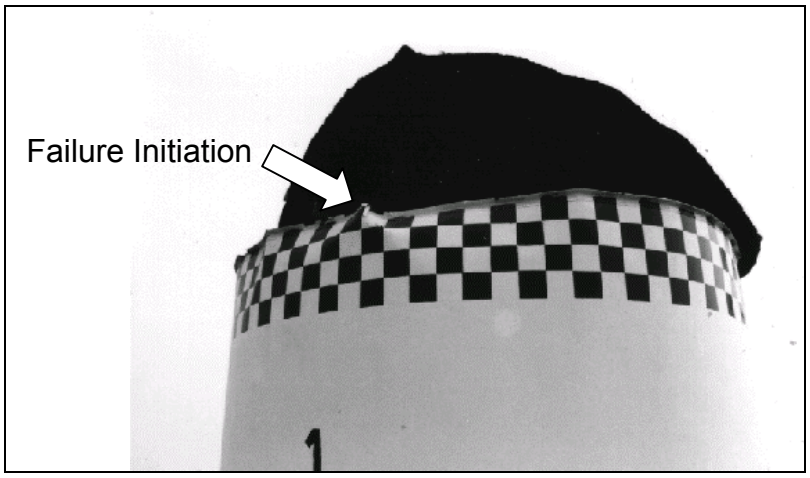

Figure 4-1: Results of tank test showing failure initiation due to local buckling (Swenson, et al., 1996)

The compressive circumferential stress in the top angle that initiates yielding is caused by the doming of the roof due to internal pressure which pulls the top angle radially inward, Figure 3-7 and Figure 3-20. Because the roof is relatively flat, this doming is effective in creating a large compression stress at relatively low pressures. Failure of the roof-to-shell is independent of tank

uplift. As the slope of the roof increases, the pressure required to cause roof-to-shell failure also increases.

The design criterion for failure of the roof-to-shell is simply the pressure at which the roof-to-shell yields. At present, this is not calculated directly in API 650, but is implied by the Area calculation in Section F.5. However, as previously discussed in Swenson et al., 1996, the area calculation in Section F.5 results in a predicted failure at a lower pressure than actually expected. In Section 5 of this report we derive new relationships for the calculation of A (compression ring area) in API 650 that result in more accurate calculation of the roof-to-shell failure pressure when buckling is not included in the analysis.

4.2 Shell-to-Bottom Joint Failure due to Yielding of Shell

In a similar manner to failure of the roof-to-shell joint, one failure mode at the shell-to-bottom joint is yielding due to compressive circumferential stresses. These stresses result from uplift of the tank that allows the bottom to "bowl," Figure 3-13 and Figure 3-23. As in failure of the roof-to-shell joint, this pulls the bottom angle radially inward, causing a compressive circumferential stress. If the average stress in the shell exceeds yielding, this yielding will result in significant deformation, increased uplift, and local buckling that will likely cause failure of the joint.

The design criterion for failure of the shell-to-bottom joint is yielding middle shell surface as a result of the pressure in the tank that causes sufficient uplift to pull the bottom of the shell radially inward and result in a high compressive circumferential stress at the joint. The assumption that failure occurs at yielding may be somewhat conservative, since, in contrast to the roof-to-shell joint where the weld is deliberately sized to be a weak joint, the welds at the shell-to-bottom joint are designed to be strong. Therefore, the large rotations and kinking that occur during failure of the roof-to-shell joint might not occur so readily at the shell-to-bottom joint.

This is a new failure condition for API 650, so there are no established guidelines for this calculation. Yielding at the shell-to-bottom joint is a function of the product level in the tank, the strength of the shell, the strength of the bottom, and the large displacement caused by tank uplift. The appendix presents a relatively simplified calculation for this pressure.

4.3 Failure of Shell-to-Bottom Joint Weld

The shell-to-bottom joint is formed by a continuous fillet weld laid on each side of the shell plate, Figure 4-2 (API 650, Section 3.1.5). In all cases, API 650 requires that the size of each weld be at least equal to the thickness of the bottom plate. With such a design, it is reasonable to assume that the bottom plate will fail before the welds, so this is not evaluated further.

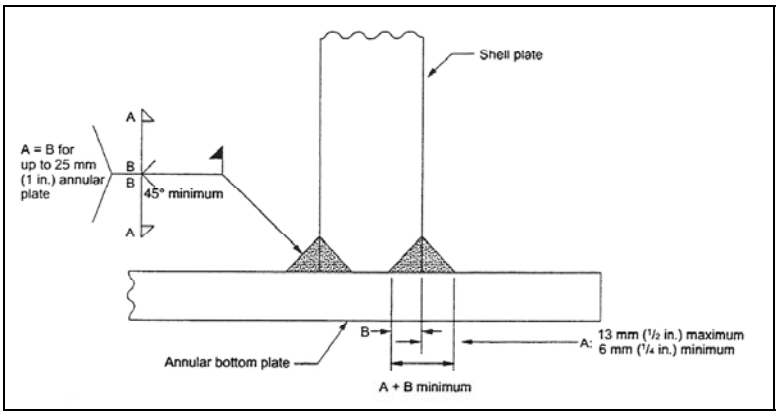

Figure 4-2: Detail of shell-to-bottom joint (API-650)

4.4 Failure of Bottom Plate Welds

Bottom plates are welded on the top side only, with a continuous full-fillet weld on all seams. Details of the bottom welds depend on whether annular plates are used. Without annular plates, the minimum distance between the shell and any three-plate laps is 12 inches. If annular plates are used, the minimum distance between the shell and any lap-welded joint on the bottom is 24 inches. During uplift, some of the bottom will be lifted off the foundation. As a result, these welds may be subjected to bending and in-plane loads that would not occur if the bottom remained flat.

In Section 5 of this report we propose criteria to prevent failure of these welds.

4.5 Failure of Attachments due to Uplift

In the event of uplift, attachments will be subjected to increased loads. This could lead to failure of the attachments or of the shell at the attachment location. This is discussed further in Section 5, although development of an appropriate criterion is left as future work.

4.6 Fracture

Failure due to fracture is not addressed in this report. It is assumed that by the selection of materials specified in API-650, sufficient toughness is provided to avoid initiation and propagation of fractures. It should be noted that there are different consequences of failure due to fracture at the roof-to-shell joint and at the shell-to-bottom joint. At the roof-to-shell joint, failure due to fracture at a pressure lower than that required for yielding would have the effect of relieving internal pressure more rapidly. This is conservative, as long as the fracture is confined to the region of the top angle. However, failure by fracture at the shell-to-bottom joint could result in bottom failure before over-pressure relief was provided by the frangible roof joint.

5. Supporting Analyses

It is impossible to test all tank designs and the behavior of the tank is sufficiently complex that a simple analysis is not possible. As a result, finite element analyses are used to establish the response of a range of tank designs to over-pressurization. The results of these analyses were used as benchmarks with which to develop approximate approaches to calculation of tank response. These approximate calculations can be used in the design process.

For simplicity, the materials at the roof-to-shell joint and the shell-to-bottom joint are assumed to have the same material properties. In some cases the lower shell and bottom can be made of materials with higher strengths, so this is a conservative assumption.

Friction between the bottom and the foundation is ignored.

It is assumed that the rafters do not affect the failure of the roof-to-shell joint. This is consistent with observations.

5.1 Designs Used for Analysis

5.1.1 Tank Size Study

Table 5-1 lists the cases used to evaluate failure for tanks with a 0.75 inch slope. These were selected to provide a range of tank sizes from 20 to 120 ft diameter and heights from 20 to 48 ft that bounded the size of tanks of interest.

Case	Dia (ft)	Height (ft)	Bottom Course (in)	Top Course (in)	Floor Thick (in)	Roof Thick (in)	Angle Width (in)	Angle Thick (in)	Liquid Level (ft)	Weight (lb)
1.a	20.0	20.0	0.1875	0.1875	0.250	0.1875	2.0	0.1875	0.0	12042
1.b	20.0	20.0	0.1875	0.1875	0.250	0.1875	2.0	0.1875	10.0	12042
1.c	20.0	20.0	0.1875	0.1875	0.250	0.1875	2.0	0.1875	19.0	12042
2.a	30.0	20.0	0.1875	0.1875	0.2500	0.1875	2.0	0.1875	0.0	19854
2.b	30.0	20.0	0.1875	0.1875	0.2500	0.1875	2.0	0.1875	10.0	19854
2.c	30.0	20.0	0.1875	0.1875	0.2500	0.1875	2.0	0.1875	19.0	19854
3.a	40.0	20.0	0.1875	0.1875	0.250	0.1875	2.0	0.2500	0.0	28960
3.b	40.0	20.0	0.1875	0.1875	0.250	0.1875	2.0	0.2500	10.0	28960
3.c	40.0	20.0	0.1875	0.1875	0.250	0.1875	2.0	0.2500	19.0	28960
4.a	30.0	32.0	0.1875	0.1875	0.2500	0.1875	2.0	0.1875	0.0	28435
4.b	30.0	32.0	0.1875	0.1875	0.2500	0.1875	2.0	0.1875	16.0	28435
4.c	30.0	32.0	0.1875	0.1875	0.2500	0.1875	2.0	0.1875	31.0	28435
5.a	40.0	32.0	0.2188	0.1875	0.250	0.1875	2.0	0.2500	0.0	41680
5.b	40.0	32.0	0.2188	0.1875	0.250	0.1875	2.0	0.2500	16.0	41680
5.c	40.0	32.0	0.2188	0.1875	0.250	0.1875	2.0	0.2500	31.0	41680
6.a	50.0	32.0	0.2500	0.2500	0.2500	0.1875	2.0	0.2500	0.0	66140
6.b	50.0	32.0	0.2500	0.2500	0.2500	0.1875	2.0	0.2500	16.0	66140
6.c	50.0	32.0	0.2500	0.2500	0.2500	0.1875	2.0	0.2500	31.0	66140
7.a	40.0	40.0	0.2500	0.1875	0.250	0.1875	2.0	0.2500	0.0	51850
7.b	40.0	40.0	0.2500	0.1875	0.250	0.1875	2.0	0.2500	20.0	51850
7.c	40.0	40.0	0.2500	0.1875	0.250	0.1875	2.0	0.2500	39.0	51850
8.a	50.0	40.0	0.2813	0.2500	0.2500	0.1875	2.0	0.2500	0.0	80441
8.b	50.0	40.0	0.2813	0.2500	0.2500	0.1875	2.0	0.2500	20.0	80441
8.c	50.0	40.0	0.2813	0.2500	0.2500	0.1875	2.0	0.2500	39.0	80441
9.a	60.0	40.0	0.3125	0.2500	0.250	0.1875	2.0	0.2500	0.0	103925
9.b	60.0	40.0	0.3125	0.2500	0.250	0.1875	2.0	0.2500	20.0	103925
9.c	60.0	40.0	0.3125	0.2500	0.250	0.1875	2.0	0.2500	39.0	103925
10.a	60.0	48.0	0.3750	0.2500	0.2500	0.1875	2.0	0.2500	0.0	126807
10.b	60.0	48.0	0.3750	0.2500	0.2500	0.1875	2.0	0.2500	24.0	126807
10.c	60.0	48.0	0.3750	0.2500	0.2500	0.1875	2.0	0.2500	47.0	126807
11.a	80.0	48.0	0.4688	0.2500	0.250	0.1875	3.0	0.3750	0.0	199829
11.b	80.0	48.0	0.4688	0.2500	0.250	0.1875	3.0	0.3750	24.0	199829
11.c	80.0	48.0	0.4688	0.2500	0.250	0.1875	3.0	0.3750	47.0	199829
12.a	100.0	48.0	0.5625	0.2500	0.2500	0.1875	3.0	0.3750	0.0	290324
12.b	100.0	48.0	0.5625	0.2500	0.2500	0.1875	3.0	0.3750	24.0	290324
12.c	100.0	48.0	0.5625	0.2500	0.2500	0.1875	3.0	0.3750	47.0	290324
13.a	120.0	48.0	0.6563	0.3125	0.250	0.1875	3.0	0.3750	0.0	412062
13.b	120.0	48.0	0.6563	0.3125	0.250	0.1875	3.0	0.3750	24.0	412062
13.c	120.0	48.0	0.6563	0.3125	0.250	0.1875	3.0	0.3750	47.0	412062

Table 5-1: Details of analyses for tanks with 0.75 inch slope

5.1.2 Roof Slope Study

Table 5-2, Table 5-3, and Table 5-4 list tank design data for slopes of 1.0, 2.0 and 3.0 inches. These analyses focused on smaller tanks, since few designs would use the steeper slopes on a large tank. In addition, these analyses only included empty and full tanks, since the proposed criteria focus on those bounding conditions.

Case	Dia (ft)	Height (ft)	Bottom Course (in)	Top Course (in)	Floor Thick (in)	Roof Thick (in)	Angle Width (in)	Angle Thick (in)	Liquid Level (ft)	Weight (lb)
101.a	20.0	20.0	0.1875	0.1875	0.250	0.1875	2.0	0.1875	0.0	12046
101.c	20.0	20.0	0.1875	0.1875	0.250	0.1875	2.0	0.1875	19.0	12046
102.a	30.0	20.0	0.1875	0.1875	0.2500	0.1875	2.0	0.1875	0.0	19862
102.c	30.0	20.0	0.1875	0.1875	0.2500	0.1875	2.0	0.1875	19.0	19862
103.a	40.0	20.0	0.1875	0.1875	0.250	0.1875	2.0	0.2500	0.0	28981
103.c	40.0	20.0	0.1875	0.1875	0.250	0.1875	2.0	0.2500	19.0	28981
104.a	30.0	32.0	0.1875	0.1875	0.2500	0.1875	2.0	0.1875	0.0	28443
104.c	30.0	32.0	0.1875	0.1875	0.2500	0.1875	2.0	0.1875	31.0	28443
105.a	40.0	32.0	0.2188	0.1875	0.250	0.1875	2.0	0.2500	0.0	41695
105.c	40.0	32.0	0.2188	0.1875	0.250	0.1875	2.0	0.2500	31.0	41695
106.a	50.0	32.0	0.2500	0.2500	0.2500	0.1875	2.0	0.2500	0.0	66162
106.c	50.0	32.0	0.2500	0.2500	0.2500	0.1875	2.0	0.2500	31.0	66162

Table 5-2: Details of analyses for tanks with 1.00 inch slope

Case	Dia (ft)	Height (ft)	Bottom Course (in)	Top Course (in)	Floor Thick (in)	Roof Thick (in)	Angle Width (in)	Angle Thick (in)	Liquid Level (ft)	Weight (lb)
201.a	20.0	20.0	0.1875	0.1875	0.250	0.1875	2.0	0.1875	0.0	12071
201.c	20.0	20.0	0.1875	0.1875	0.250	0.1875	2.0	0.1875	19.0	12071
202.a	30.0	20.0	0.1875	0.1875	0.2500	0.1875	2.0	0.1875	0.0	19918
202.c	30.0	20.0	0.1875	0.1875	0.2500	0.1875	2.0	0.1875	19.0	19918
203.a	40.0	20.0	0.1875	0.1875	0.250	0.1875	2.0	0.2500	0.0	29079
203.c	40.0	20.0	0.1875	0.1875	0.250	0.1875	2.0	0.2500	19.0	29079
204.a	30.0	32.0	0.1875	0.1875	0.2500	0.1875	2.0	0.1875	0.0	28498
204.c	30.0	32.0	0.1875	0.1875	0.2500	0.1875	2.0	0.1875	31.0	28498
205.a	40.0	32.0	0.2188	0.1875	0.250	0.1875	2.0	0.2500	0.0	41793
205.c	40.0	32.0	0.2188	0.1875	0.250	0.1875	2.0	0.2500	31.0	41793
206.a	50.0	32.0	0.2500	0.2500	0.2500	0.1875	2.0	0.2500	0.0	66316
206.c	50.0	32.0	0.2500	0.2500	0.2500	0.1875	2.0	0.2500	31.0	66316

Table 5-3: Details of analyses for tanks with 2.00 inch slope

Case	Dia (ft)	Height (ft)	Bottom Course (in)	Top Course (in)	Floor Thick (in)	Roof Thick (in)	Angle Width (in)	Angle Thick (in)	Liquid Level (ft)	Weight (lb)
301.a	20.0	20.0	0.1875	0.1875	0.250	0.1875	2.0	0.1875	0.0	12111
301.c	20.0	20.0	0.1875	0.1875	0.250	0.1875	2.0	0.1875	19.0	12111
302.a	30.0	20.0	0.1875	0.1875	0.2500	0.1875	2.0	0.1875	0.0	20009
302.c	30.0	20.0	0.1875	0.1875	0.2500	0.1875	2.0	0.1875	19.0	20009
303.a	40.0	20.0	0.1875	0.1875	0.250	0.1875	2.0	0.2500	0.0	29241
303.c	40.0	20.0	0.1875	0.1875	0.250	0.1875	2.0	0.2500	19.0	29241
304.a	30.0	32.0	0.1875	0.1875	0.2500	0.1875	2.0	0.1875	0.0	28589
304.c	30.0	32.0	0.1875	0.1875	0.2500	0.1875	2.0	0.1875	31.0	28589
305.a	40.0	32.0	0.2188	0.1875	0.250	0.1875	2.0	0.2500	0.0	41955
305.c	40.0	32.0	0.2188	0.1875	0.250	0.1875	2.0	0.2500	31.0	41955
306.a	50.0	32.0	0.2500	0.2500	0.2500	0.1875	2.0	0.2500	0.0	66569
306.c	50.0	32.0	0.2500	0.2500	0.2500	0.1875	2.0	0.2500	31.0	66569

Table 5-4: Details of analyses for tanks with 3.00 inch slope

5.1.3 Roof Thickness Study

Table 5-5 gives the parameters of the tanks used to evaluate the effect of roof thickness on failure pressure. For this study, the tank dimensions remained the same, but the roof thickness was varied from 3/16 to 5/16 inch.

Case	Dia (ft)	Height (ft)	Bottom Course (in)	Top Course (in)	Floor Thick (in)	Roof Thick (in)	Angle Width (in)	Angle Thick (in)	Liquid Level (ft)	Weight (lb)
roof_3_16	30.0	32.0	0.1875	0.1875	0.2500	0.1875	2.0	0.1875	31.0	28435
roof_4_16	30.0	32.0	0.1875	0.1875	0.2500	0.2500	2.0	0.1875	31.0	30246
roof_5_16	30.0	32.0	0.1875	0.1875	0.2500	0.3125	2.0	0.1875	31.0	32057

Table 5-5: Details of designs used for roof thickness study

5.1.4 Roof Attachment Study

API-650 allows different configurations for attachment of the roof to the top angle and the angle to the shell. The angle can either face in or out of the tank and the angle can either overlap the top of the shell or be an extension to the shell. Table 5-6 gives the cases used to examine the sensitivity to these options. Again, the size of the tank was kept constant and only the angle attachment was varied.

Case	Dia (ft)	Height (ft)	Bottom Course (in)	Top Course (in)	Floor Thick (in)	Roof Thick (in)	Angle Width (in)	Angle Thick (in)	Angle Orient	Angle Overlap	Liquid Level (ft)	Weight (lb)
Attach-1	30.0	32.0	0.1875	0.1875	0.2500	0.1875	2.0	0.1875	out	no	31.0	28435
Attach-2	30.0	32.0	0.1875	0.1875	0.2500	0.1875	2.0	0.1875	in	no	31.0	28316
Attach-3	30.0	32.0	0.1875	0.1875	0.2500	0.1875	2.0	0.1875	out	yes	31.0	28532
Attach-4	30.0	32.0	0.1875	0.1875	0.2500	0.1875	2.0	0.1875	in	yes	31.0	32057

Table 5-6: Cases used to examine the significance of roof attachment detail

5.1.5 Bottom Thickness Study

This study examined the effects of changing the bottom thickness

Case	Dia (ft)	Height (ft)	Bottom Course (in)	Top Course (in)	Floor Thick (in)	Roof Thick (in)	Angle Width (in)	Angle Thick (in)	Liquid Level (ft)	Weight (lb)
floor_1_8.a	30.0	32.0	0.1875	0.1875	0.1250	0.1875	2.0	0.1875	0.0	28435
floor_1_8.b	30.0	32.0	0.1875	0.1875	0.1250	0.1875	2.0	0.1875	16.0	28435
floor_1_8.c	30.0	32.0	0.1875	0.1875	0.1250	0.1875	2.0	0.1875	31.0	28435
floor_2_8.a	30.0	32.0	0.1875	0.1875	0.2500	0.1875	2.0	0.1875	0.0	28435
floor_2_8.b	30.0	32.0	0.1875	0.1875	0.2500	0.1875	2.0	0.1875	16.0	28435
floor_2_8.c	30.0	32.0	0.1875	0.1875	0.2500	0.1875	2.0	0.1875	31.0	28435
floor_3_8.a	30.0	32.0	0.1875	0.1875	0.3750	0.1875	2.0	0.1875	0.0	28435
floor_3_8.b	30.0	32.0	0.1875	0.1875	0.3750	0.1875	2.0	0.1875	16.0	28435
floor_3_8.c	30.0	32.0	0.1875	0.1875	0.3750	0.1875	2.0	0.1875	31.0	28435

5.1.6 Yield Stress Variation Study

For all of the other calculations reported, the minimum yield strength was assumed to be 36 ksi. This study looked at the effect of other yield strengths.

Case	Dia (ft)	Height (ft)	Bottom Course (in)	Top Course (in)	Floor Thick (in)	Roof Thick (in)	Angle Width (in)	Angle Thick (in)	Liquid Level (ft)	Weight (lb)	Yield Stress ksi)
ys_36.a	30.0	32.0	0.1875	0.1875	0.2500	0.1875	2.0	0.1875	0.0	28435	36
ys_36.b	30.0	32.0	0.1875	0.1875	0.2500	0.1875	2.0	0.1875	16.0	28435	36
ys_36.c	30.0	32.0	0.1875	0.1875	0.2500	0.1875	2.0	0.1875	31.0	28435	36
ys_48.a	30.0	32.0	0.1875	0.1875	0.2500	0.1875	2.0	0.1875	0.0	28435	48
ys_48.b	30.0	32.0	0.1875	0.1875	0.2500	0.1875	2.0	0.1875	16.0	28435	48
ys_48.c	30.0	32.0	0.1875	0.1875	0.2500	0.1875	2.0	0.1875	31.0	28435	48
ys_60.a	30.0	32.0	0.1875	0.1875	0.2500	0.1875	2.0	0.1875	0.0	28435	60
ys_60.b	30.0	32.0	0.1875	0.1875	0.2500	0.1875	2.0	0.1875	16.0	28435	60
ys_60.c	30.0	32.0	0.1875	0.1875	0.2500	0.1875	2.0	0.1875	31.0	28435	60

Table 5-7: Design parameters for yield strength study

5.2 Static Large Displacement, Elastic Calculations

SafeRoof version 2.1 offers two options for tank analysis:

- Elastic, large displacement, static finite element analysis with and without buckling in the roof and floor, and
- Inelastic, large displacement, dynamic finite element analysis. This uses the FMA-3D code (FMA, 2003) which has been integrated into SafeRoof.

For both options, nonlinear contact elements are used to support the tank on the foundation and to support the roof on rafters when the internal pressure is not sufficient to lift the roof.

Results are presented for both types of analyses. The results for the large deformation, elastic calculations made with SafeRoof are summarized in Table 5-8, Table 5-9 Table 5-10, Table 5-11, and Table 5-12.

In these tables:

- "First Uplift" is the pressure at incipient tank uplift,
- P_{top} is the pressure at which the roof-to-shell joint fails,
- P_{bot} is the pressure at which the shell-to-bottom joint fails,
- "Uplift R" is the radius at which the bottom is lifted above the foundation,
- "Uplift" is the magnitude of the uplift displacement of the bottom of the shell,
- "Joint Failure Ratio" is the ratio of the pressure to fail the shell-to-bottom joint divided by the pressure to fail the roof-to-shell joint. The larger the number, the more certain it is that the frangible roof will relieve tank over-pressurization before any other failure.
- "Floor Sig T" is the circumferential stress in the bottom at the shell-to-bottom joint.
- "Floor Sig R" is the radial stress in the bottom at the shell-to-bottom joint.

In addition, most of the tables provide results for pressures that are 1.5 and 2.5 times the roof-to-shell joint failure pressure. As will be discussed, these two factors correspond to the suggested failure ratios for empty and full tanks, respectively.

In these tables, results that do not meet the possible failure criteria have been highlighted. Joint Failure Ratios less than 1.5 for empty tanks and 2.5 for full tanks are flagged in gray. Uplift

displacements greater than 4.0 inches are flagged in gray (note this is just done to highlight results, this is not a suggested design criterion). Stresses greater than the yield stress (14,760 psi) are flagged in gray (based on the weld strength analysis provided in the Appendix).

5.2.1 Tank Size Study

Table 5-8 and Table 5-9 give the details of the results for the tank size study. This same data is plotted in Figure 5-1, Figure 5-2, and Figure 5-3. Figure 5-4 gives the average uplift at the top joint failure pressure. The data is shown plotted both on linear and logarithmic axes. In all figures, the solid lines represent the top joint failure pressures, long dashed lines represent bottom failure pressures, and the short dashed lines represent balanced uplift pressures.

These figures illustrate the following key observations:

- For empty tanks, Figure 5-1, the top and bottom failure pressures are quite close together, especially for smaller tanks. For a 20 ft diameter tank with a height of 20 ft, the top joint failure pressure is 1.92 psi and the bottom joint failure pressure is 2.04 psi without considering buckling and 1.49 psi and 1.68 psi with buckling considered. In both cases, the pressures for failure of the top joint are so close to the failure pressures for the bottom joint, that it is possible for both failures to occur essentially simultaneously.
- For full tanks, the weight of the contents protects against bottom uplift, so the failure pressures at the bottom become 3.84 psi and 3.82 psi, respectively. This means that failure is more likely to occur at the top joint.
- For large tanks, both empty and full, the top joint is significantly weaker than the bottom joint.
- Significant uplift can occur before top joint failure, especially for smaller empty tanks.

When plotted using log-log axes, the curves for top failure become very linear. The curves for bottom failure are close to linear. The bottom uplift pressure is not linear. The fact that the failure pressures are linear on log-log plots might provide an alternate estimate of the failure pressures for different tanks.

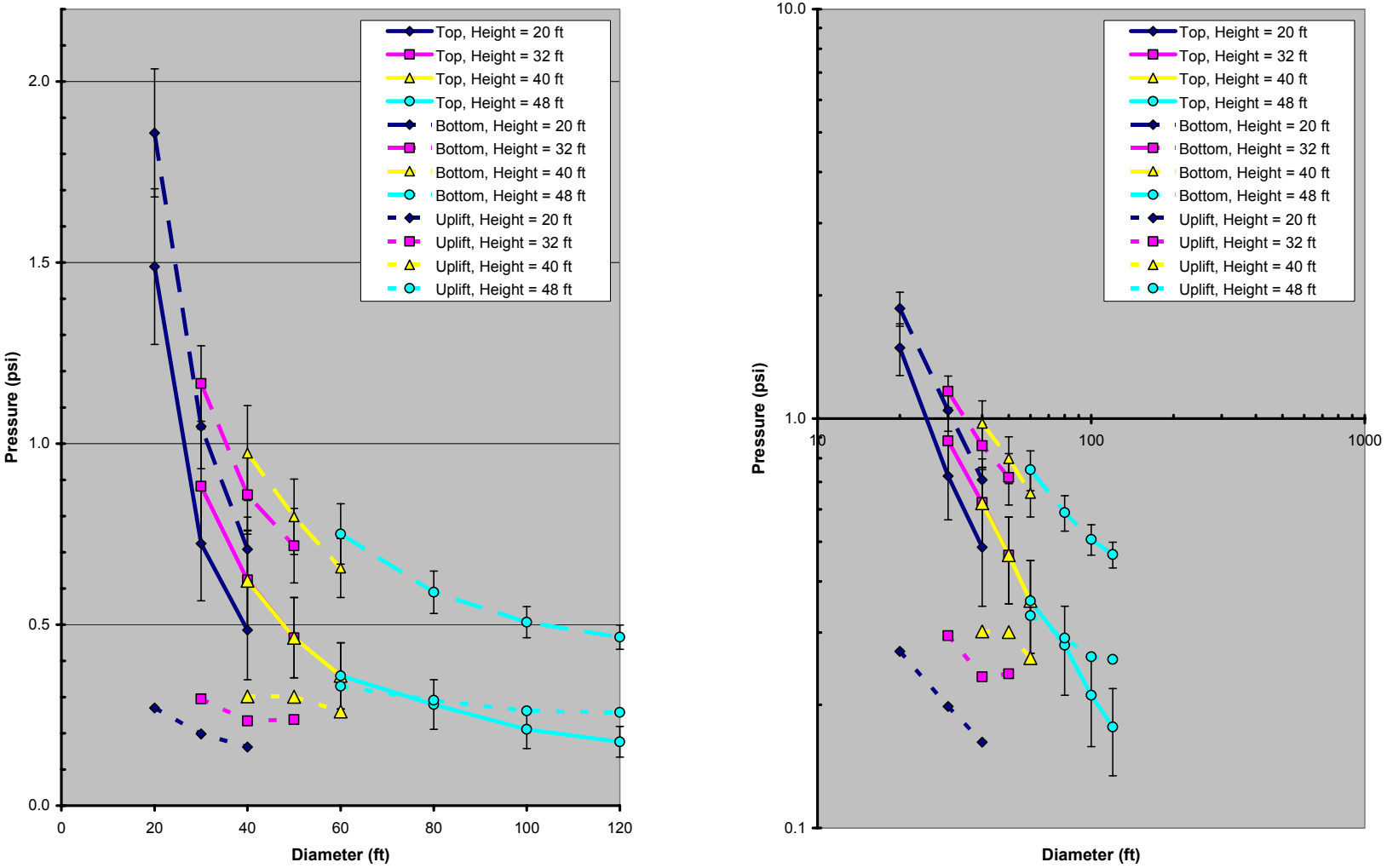

a. Linear axes

b. Logarithmic axes

Figure 5-1: Empty tanks - failure pressures for top (roof-to-shell) and bottom (shell-to-floor) joints and balanced uplift pressure. Graph lines drawn at average of solutions with and without buckling, error bars indicate bounds.

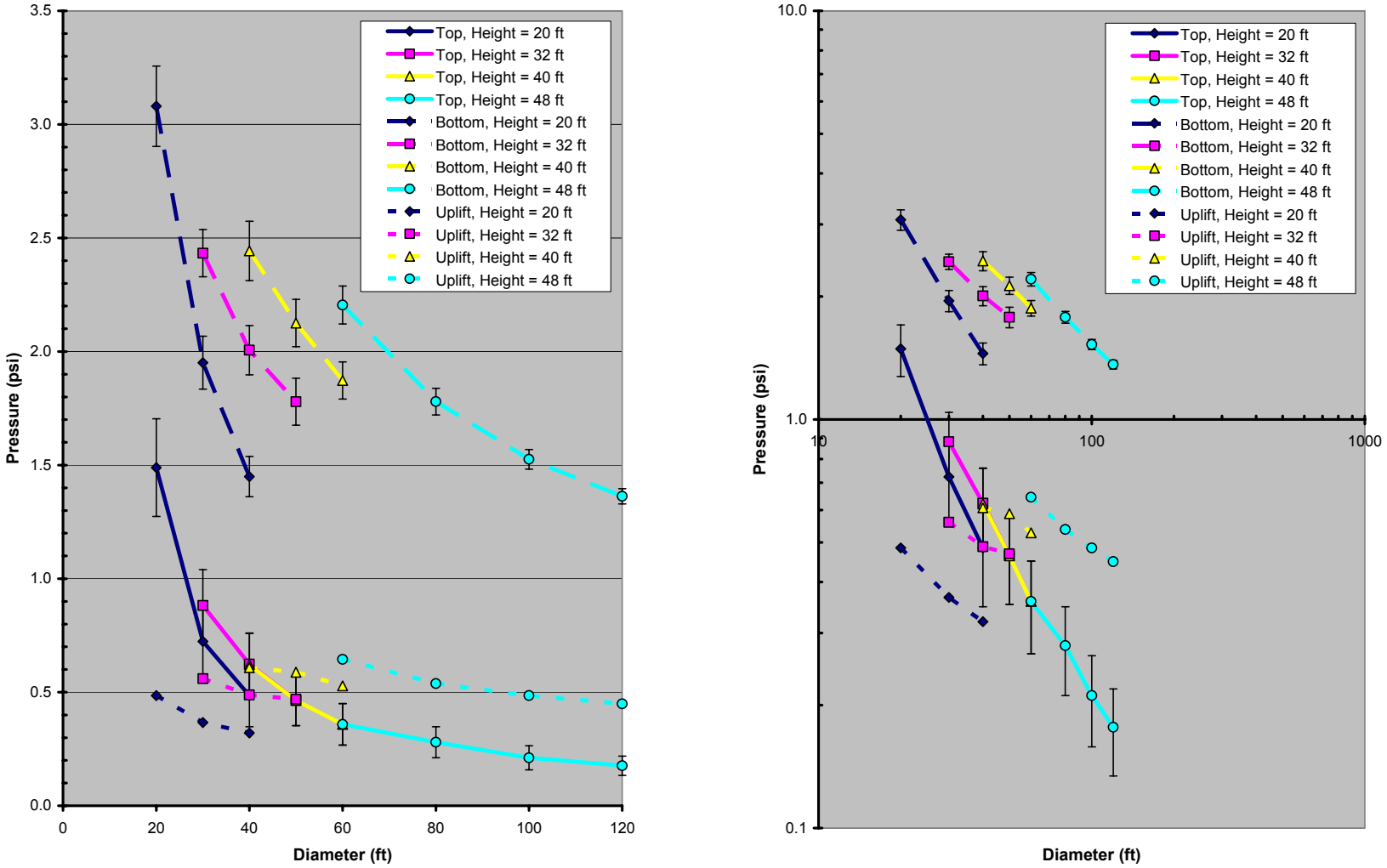

a. Linear axes

b. Logarithmic axes

Figure 5-2: Half-full tanks, failure pressures for top (roof-to-shell) and bottom (shell-to-floor) joints and balanced uplift pressure. Graph lines drawn at average of solutions with and without buckling, error bars indicate bounds.

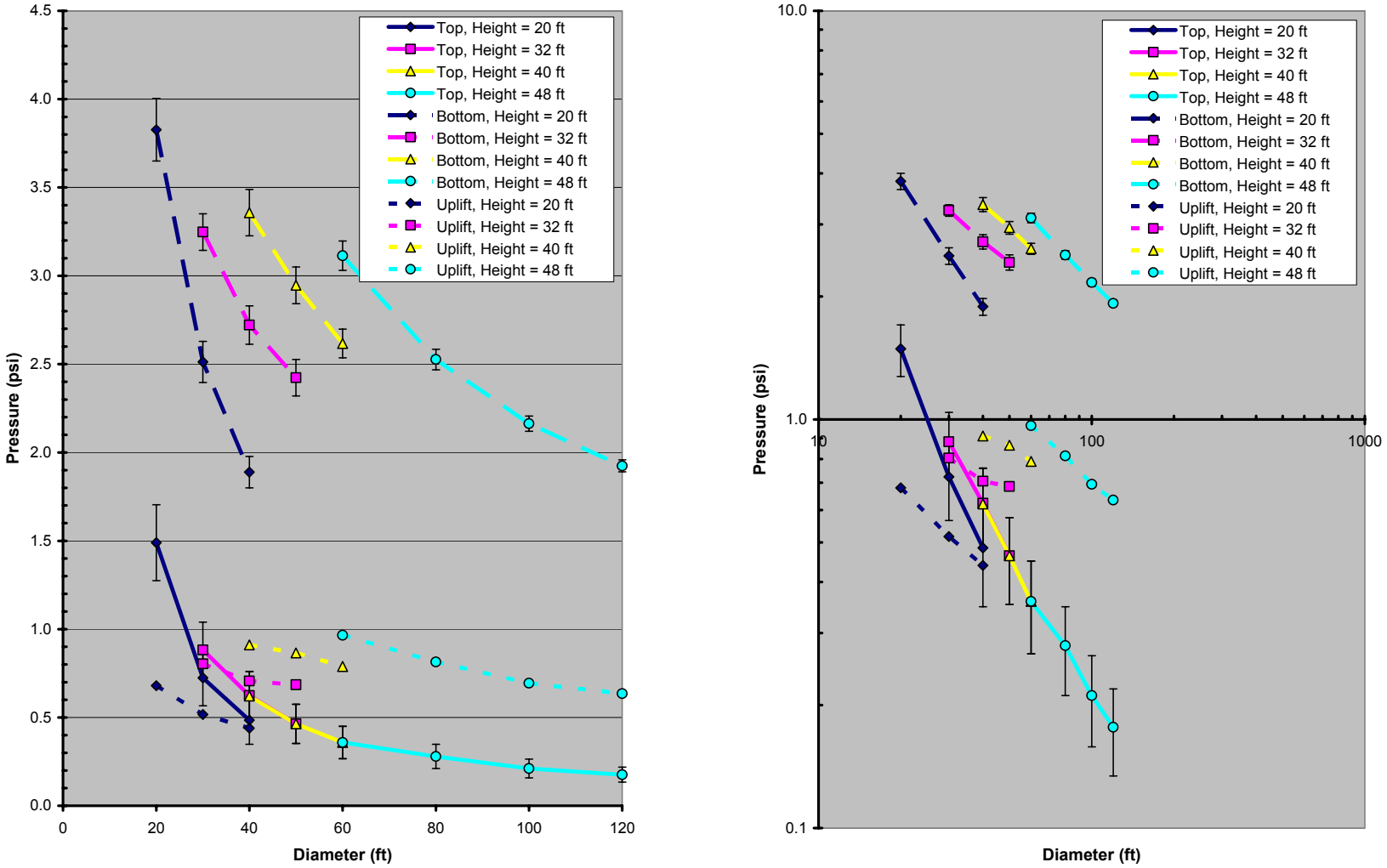

a. Linear axes

b. Logarithmic axes

Figure 5-3: Full tanks, failure pressures for top (roof-to-shell) and bottom (shell-to-floor) joints and balanced uplift pressure. Graph lines drawn at average of solutions with and without buckling, error bars indicate bounds.

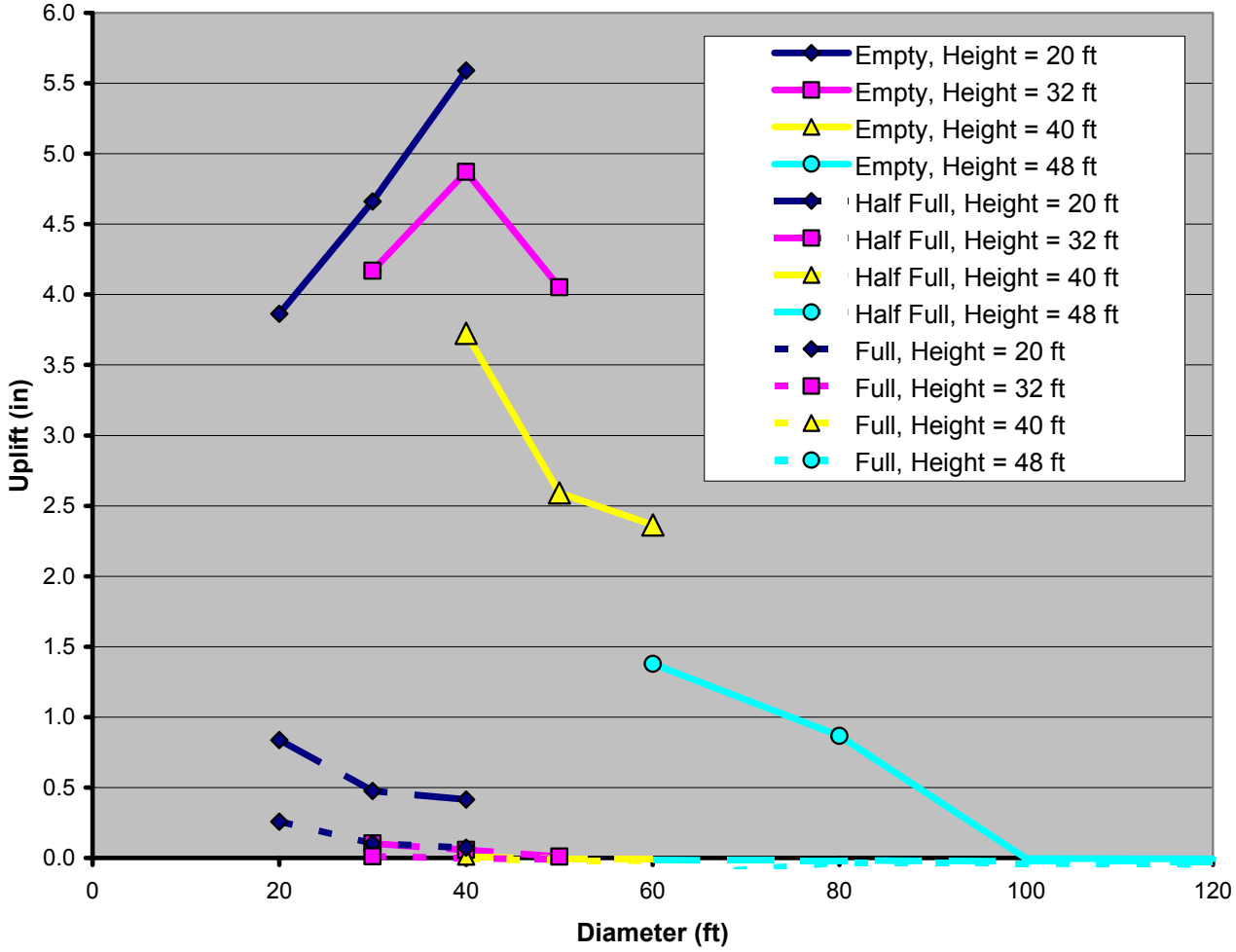

Figure 5-4: Average uplift at top joint failure pressure

Case	Dia (ft)	Height (ft)	Liquid Level (ft)	First Uplift (psi)	Top Joint Failure			Bottom Joint Failure			Joint Failure Ratio	P1.5 (Empty) P2.5 (Full)					
					Ptop (psi)	Uplift R (in)	Uplift (in)	P (psi)	Uplift R (in)	Uplift (in)		P (psi)	Uplift R (in)	R-Rup (in)	Uplift (in)	Floor SigT (psi)	Floor SigR (psi)
1.a	20.0	20.0	0.0	0.270	1.919	50.0	3.984	2.035	46.0	4.131	1.06	2.879	42.0	78.0	5.044	-43280	2140
1.b	20.0	20.0	10.0	0.485	1.920	99.0	1.126	3.118	91.0	2.493	1.62						
1.c	20.0	20.0	19.0	0.680	1.919	108.5	0.379	3.838	97.0	2.088	2.00	4.798	95.0	25.0	2.782	-37400	1760
2.a	30.0	20.0	0.0	0.198	1.040	86.0	5.327	1.164	81.0	5.759	1.12	1.560	75.0	105.0	6.926	-43010	1460
2.b	30.0	20.0	10.0	0.367	1.045	161.0	0.786	1.969	148.5	3.129	1.88						
2.c	30.0	20.0	19.0	0.517	1.045	171.5	0.178	2.521	155.0	2.660	2.41	2.613	155.0	25.0	2.809	-26520	800
3.a	40.0	20.0	0.0	0.162	0.693	129.0	6.481	0.797	123.0	7.216	1.15	1.040	111.0	129.0	8.652	-43030	1070
3.b	40.0	20.0	10.0	0.319	0.692	223.5	0.521	1.462	205.5	3.702	2.11						
3.c	40.0	20.0	19.0	0.438	0.692	233.5	0.082	1.892	213.0	3.122	2.73	1.730	215.0	25.0	2.653	-18460	700
4.a	30.0	32.0	0.0	0.295	1.040	98.0	4.684	1.270	90.0	5.512	1.22	1.560	81.0	99.0	6.388	-39980	1360
4.b	30.0	32.0	16.0	0.560	1.045	170.5	0.185	2.437	153.0	2.758	2.33						
4.c	30.0	32.0	31.0	0.804	1.046	176.3	0.027	3.255	161.0	2.346	3.11	2.615	163.5	16.5	1.436	-9630	1400
5.a	40.0	32.0	0.0	0.234	0.695	146.0	5.382	0.967	129.0	7.248	1.39	1.043	123.0	117.0	7.682	-37190	1090
5.b	40.0	32.0	16.0	0.488	0.695	233.5	0.062	2.021	211.0	3.582	2.91						
5.c	40.0	32.0	31.0	0.706	0.691	238.3	-0.001	2.720	217.0	3.049	3.94	1.728	225.5	14.5	0.921	-3140	710
6.a	50.0	32.0	0.0	0.238	0.575	210.0	5.966	0.821	177.0	8.643	1.43	0.863	171.0	129.0	9.030	-37600	1000
6.b	50.0	32.0	16.0	0.469	0.576	294.7	0.026	1.797	268.5	4.369	3.12						
6.c	50.0	32.0	31.0	0.685	0.577	299.3	-0.005	2.427	275.0	3.757	4.21	1.443	285.5	14.5	0.881	-2090	730
7.a	40.0	40.0	0.0	0.302	0.693	158.0	4.510	1.105	135.0	7.283	1.59	1.040	135.0	105.0	6.921	-32660	1030
7.b	40.0	40.0	20.0	0.608	0.694	236.3	0.010	2.462	211.0	3.653	3.55						
7.c	40.0	40.0	39.0	0.911	0.695	239.3	-0.007	3.371	219.0	3.155	4.85	1.738	230.5	9.5	0.393	-410	670
8.a	50.0	40.0	0.0	0.301	0.575	214.0	4.848	0.902	177.0	8.444	1.57	0.863	183.0	117.0	8.092	-33060	1030
8.b	50.0	40.0	20.0	0.588	0.576	297.2	-0.001	2.143	268.5	4.365	3.72						
8.c	50.0	40.0	39.0	0.865	0.576	298.3	-0.012	2.953	275.0	3.816	5.13	1.440	290.5	9.5	0.340	-70	570
9.a	60.0	40.0	0.0	0.260	0.450	278.0	4.728	0.738	231.0	9.597	1.64	0.675	237.0	123.0	8.725	-30440	920
9.b	60.0	40.0	20.0	0.528	0.450	361.3	-0.005	1.890	325.5	5.052	4.20						
9.c	60.0	40.0	39.0	0.789	0.450	358.3	-0.017	2.631	333.0	4.461	5.85	1.125	351.5	8.5	0.177	320	500
10.a	60.0	48.0	0.0	0.330	0.450	298.0	2.758	0.834	231.0	9.470	1.85	0.675	255.0	105.0	7.285	-24330	880
10.b	60.0	48.0	24.0	0.645	0.450	361.8	-0.009	2.228	328.5	5.091	4.95						
10.c	60.0	48.0	47.0	0.950	0.450	357.8	-0.230	3.129	335.0	4.524	6.95	1.125	355.2	4.8	0.030	510	530
11.a	80.0	48.0	0.0	0.291	0.315	448.5	0.266	0.648	333.0	11.690	2.06	0.473	375.0	105.0	7.102	-17860	670
11.b	80.0	48.0	24.0	0.537	0.315	481.3	-0.015	1.794	445.5	6.048	5.70						
11.c	80.0	48.0	47.0	0.812	0.315	478.8	-0.031	2.541	451.0	5.429	8.07	0.788	475.7	4.3	-0.002	590	580
12.a	100.0	48.0	0.0	0.261	0.241	600.3	-0.001	0.549	438.0	13.768	2.28	0.362	510.0	90.0	5.626	-10240	440
12.b	100.0	48.0	24.0	0.484	0.241	601.8	-0.020	1.535	562.5	6.956	6.37						
12.c	100.0	48.0	47.0	0.693	0.241	598.3	-0.380	2.177	568.5	6.266	9.03	0.603	595.8	4.2	-0.012	670	650
13.a	120.0	48.0	0.0	0.258	0.212	720.3	-0.004	0.499	546.0	15.646	2.35	0.318	642.0	78.0	4.139	-5290	260
13.b	120.0	48.0	24.0	0.448	0.212	721.3	-0.023	1.372	679.5	7.847	6.47						
13.c	120.0	48.0	47.0	0.635	0.211	717.3	-0.042	1.930	688.5	6.998	9.15	0.528	715.3	4.7	-0.016	750	720

Table 5-8: Results for tanks with 0.75 inch slope without buckling (cells highlighted in gray indicate failure to meet possible design criteria)

Case	Dia (ft)	Height (ft)	Liquid Level (ft)	First Uplift (psi)	Top Joint Failure			Bottom Joint Failure			Joint Failure Ratio
					Ptop (psi)	Uplift R (in)	Uplift (in)	P (psi)	Uplift R (in)	Uplift (in)	
B1.a	20.0	20.0	0.0	0.270	1.489	54.0	3.864	1.681	50.0	4.217	1.13
B1.b	20.0	20.0	10.0	0.485	1.496	103.5	0.550	3.042	91.0	2.500	2.03
B1.c	20.0	20.0	19.0	0.680	1.496	112.5	0.137	3.816	97.0	2.101	2.55
B2.a	30.0	20.0	0.0	0.198	0.724	98.0	4.662	0.931	90.0	5.808	1.29
B2.b	30.0	20.0	10.0	0.367	0.724	169.5	0.168	1.933	148.5	3.135	2.67
B2.c	30.0	20.0	19.0	0.517	0.723	175.3	0.028	2.505	155.0	2.661	3.46
B3.a	40.0	20.0	0.0	0.162	0.485	146.0	5.592	0.619	135.0	7.185	1.28
B3.b	40.0	20.0	10.0	0.320	0.484	231.5	0.079	1.437	205.5	3.715	2.97
B3.c	40.0	20.0	19.0	0.439	0.484	237.3	0.004	1.885	213.0	3.136	3.89
B4.a	30.0	32.0	0.0	0.295	0.724	110.0	3.653	1.062	98.0	5.584	1.47
B4.b	30.0	32.0	16.0	0.560	0.725	175.8	0.022	2.429	153.0	2.783	3.35
B4.c	30.0	32.0	31.0	0.804	0.726	179.3	-0.002	3.241	161.0	2.336	4.46
B5.a	40.0	32.0	0.0	0.234	0.486	166.0	3.862	0.750	141.0	6.999	1.54
B5.b	40.0	32.0	16.0	0.488	0.486	237.8	0.000	1.991	211.0	3.566	4.10
B5.c	40.0	32.0	31.0	0.706	0.486	241.3	-0.007	2.723	217.0	3.075	5.60
B6.a	50.0	32.0	0.0	0.238	0.353	242.0	2.138	0.615	195.0	8.010	1.74
B6.b	50.0	32.0	16.0	0.469	0.353	300.3	-0.005	1.761	268.5	4.364	4.99
B6.c	50.0	32.0	31.0	0.685	0.353	301.3	-0.013	2.421	275.0	3.789	6.86
B7.a	40.0	40.0	0.0	0.302	0.483	182.0	2.411	0.843	146.0	6.777	1.75
B7.b	40.0	40.0	20.0	0.608	0.483	240.8	-0.004	2.435	211.0	3.655	5.04
B7.c	40.0	40.0	39.0	0.911	0.482	236.3	-0.013	3.360	217.0	3.156	6.97
B8.a	50.0	40.0	0.0	0.301	0.353	268.5	0.335	0.694	195.0	7.809	1.97
B8.b	50.0	40.0	20.0	0.588	0.353	300.8	-0.009	2.108	268.5	4.366	5.97
B8.c	50.0	40.0	39.0	0.865	0.352	295.3	-0.019	2.940	275.0	3.827	8.35
B9.a	60.0	40.0	0.0	0.260	0.267	356.7	0.000	0.575	249.0	8.875	2.15
B9.b	60.0	40.0	20.0	0.528	0.267	360.8	-0.012	1.855	325.5	5.041	6.95
B9.c	60.0	40.0	39.0	0.789	0.267	353.5	-0.024	2.603	333.0	4.432	9.75
B10.a	60.0	48.0	0.0	0.330	0.267	360.3	-0.002	0.667	255.0	8.722	2.50
B10.b	60.0	48.0	24.0	0.645	0.267	361.3	-0.017	2.182	328.5	5.046	8.17
B10.c	60.0	48.0	47.0	0.966	0.267	353.5	-0.030	3.099	335.0	4.498	11.61
B11.a	80.0	48.0	0.0	0.291	0.211	480.3	-0.004	0.531	357.0	10.643	2.52
B11.b	80.0	48.0	24.0	0.538	0.211	480.8	-0.021	1.765	445.5	6.020	8.36
B11.c	80.0	48.0	47.0	0.814	0.211	482.3	-0.037	2.512	453.0	5.372	11.91
B12.a	100.0	48.0	0.0	0.262	0.158	600.3	-0.007	0.464	465.0	12.568	2.94
B12.b	100.0	48.0	24.0	0.485	0.158	600.8	-0.025	1.516	562.5	6.936	9.59
B12.c	100.0	48.0	47.0	0.694	0.158	602.3	-0.043	2.153	571.0	6.191	13.63
B13.a	120.0	48.0	0.0	0.258	0.134	705.5	-0.010	0.432	573.0	14.382	3.22
B13.b	120.0	48.0	24.0	0.449	0.134	721.3	-0.029	1.354	679.5	7.796	10.10
B13.c	120.0	48.0	47.0	0.635	0.133	722.8	-0.048	1.918	688.5	6.971	14.42

Table 5-9: Results for tanks with 0.75 inch slope with buckling (cells highlighted in gray indicate failure to meet possible design criteria)

5.2.2 Roof Slope Study

Table 5-10, Table 5-11, and Table 5-12 give results for the study of roof slope.

Case	Dia (ft)	Height (ft)	Liquid Level (ft)	First Uplift (psi)	Top Failure			Bottom Failure			Joint Failure Ratio
					Ptop (psi)	Uplift R (in)	Uplift (in)	Pbot (psi)	Uplift R (in)	Uplift (in)	
101.a	20.0	20.0	0.0	0.270	2.100	46.0	4.213	2.040	46.0	4.137	0.97
101.c	20.0	20.0	19.0	0.680	2.117	106.5	0.533	3.860	97.0	2.088	1.82
102.a	30.0	20.0	0.0	0.198	1.142	81.0	5.685	1.164	81.0	5.758	1.02
102.c	30.0	20.0	19.0	0.517	1.145	169.5	0.271	2.521	155.0	2.659	2.20
103.a	40.0	20.0	0.0	0.162	0.833	117.0	7.439	0.798	123.0	7.214	0.96
103.c	40.0	20.0	19.0	0.438	0.832	230.5	0.229	1.889	215.0	3.111	2.27
104.a	30.0	32.0	0.0	0.295	1.148	94.0	5.091	1.270	90.0	5.512	1.11
104.c	30.0	32.0	31.0	0.804	1.149	175.3	0.048	3.251	161.0	2.339	2.83
105.a	40.0	32.0	0.0	0.234	0.832	135.0	6.379	0.967	129.0	7.245	1.16
105.c	40.0	32.0	31.0	0.706	0.832	236.3	0.015	2.725	217.0	3.059	3.28
106.a	50.0	32.0	0.0	0.238	0.631	195.0	6.660	0.821	177.0	8.642	1.30
106.c	50.0	32.0	31.0	0.685	0.632	298.2	-0.003	2.427	275.0	3.756	3.84

Table 5-10: Results for tanks with 1.0 inch slope (cells highlighted in gray indicate failure to meet possible design criteria)

Case	Dia (ft)	Height (ft)	Liquid Level (ft)	First Uplift (psi)	Top Failure			Bottom Failure			Joint Failure Ratio
					Ptop (psi)	Uplift R (in)	Uplift (in)	Pbot (psi)	Uplift R (in)	Uplift (in)	
201.a	20.0	20.0	0.0	0.270	2.843	42.0	5.010	2.040	46.0	4.136	0.72
201.c	20.0	20.0	19.0	0.680	2.849	102.5	1.217	3.847	97.0	2.096	1.35
202.a	30.0	20.0	0.0	0.198	1.535	75.0	6.858	1.166	81.0	5.759	0.76
202.c	30.0	20.0	19.0	0.517	1.535	164.5	0.830	2.521	155.0	2.658	1.64
203.a	40.0	20.0	0.0	0.162	1.120	105.0	9.052	0.798	123.0	7.210	0.71
203.c	40.0	20.0	19.0	0.438	1.119	224.5	0.809	1.893	213.0	3.123	1.69
204.a	30.0	32.0	0.0	0.295	1.534	81.0	6.313	1.271	90.0	5.511	0.83
204.c	30.0	32.0	31.0	0.804	1.535	172.5	0.193	3.254	161.0	2.342	2.12
205.a	40.0	32.0	0.0	0.234	1.120	117.0	8.088	0.968	129.0	7.243	0.86
205.c	40.0	32.0	31.0	0.706	1.120	233.5	0.118	2.724	217.0	3.054	2.43
206.a	50.0	32.0	0.0	0.238	0.843	171.0	8.837	0.821	177.0	8.648	0.97
206.c	50.0	32.0	31.0	0.685	0.842	295.2	0.031	2.426	275.0	3.753	2.88

Table 5-11: Results for tanks with 2.0 inch slope (cells highlighted in gray indicate failure to meet possible design criteria)

Case	Dia (ft)	Height (ft)	Liquid Level (ft)	First Uplift (psi)	Top Failure			Bottom Failure			Joint Failure Ratio
					Ptop (psi)	Uplift R (in)	Uplift (in)	Pbot (psi)	Uplift R (in)	Uplift (in)	
301.a	20.0	20.0	0.0	0.270	3.569	38.0	5.643	2.051	46.0	4.147	0.57
301.c	20.0	20.0	19.0	0.680	3.574	99.0	1.872	3.849	97.0	2.096	1.08
302.a	30.0	20.0	0.0	0.198	1.915	69.0	7.781	1.167	81.0	5.756	0.61
302.c	30.0	20.0	19.0	0.517	1.910	161.0	1.543	2.522	155.0	2.658	1.32
303.a	40.0	20.0	0.0	0.162	1.401	99.0	10.331	0.800	123.0	7.206	0.57
303.c	40.0	20.0	19.0	0.438	1.399	221.0	1.634	1.895	213.0	3.123	1.35
304.a	30.0	32.0	0.0	0.295	1.915	75.0	7.285	1.272	90.0	5.511	0.66
304.c	30.0	32.0	31.0	0.804	1.916	168.5	0.517	3.253	161.0	2.340	1.70
305.a	40.0	32.0	0.0	0.234	1.401	111.0	9.420	0.970	129.0	7.239	0.69
305.c	40.0	32.0	31.0	0.706	1.401	229.5	0.388	2.726	217.0	3.056	1.95
306.a	50.0	32.0	0.0	0.238	1.052	159.0	10.551	0.822	177.0	8.643	0.78
306.c	50.0	32.0	31.0	0.685	1.051	291.5	0.179	2.428	275.0	3.754	2.31

Table 5-12: Results for tanks with 3.0 inch slope (cells highlighted in gray indicate failure to meet possible design criteria)

5.2.3 Roof Thickness Study

The results for the roof thickness study are given in Table 5-13 and plotted in Figure 5-5. The results show an approximately linear dependence of failure of the top joint with the thickness of the roof.

Case	Dia (ft)	Height (ft)	Bottom Course (in)	Top Course (in)	Floor Thick (in)	Roof Thick (in)	Angle Width (in)	Angle Thick (in)	Liquid Level (ft)	Weight (lb)	Top Failure (psi)
roof_3_16	30.0	32.0	0.1875	0.1875	0.2500	0.1875	2.0	0.1875	31.0	28435	1.043
roof_4_16	30.0	32.0	0.1875	0.1875	0.2500	0.2500	2.0	0.1875	31.0	30246	1.357
roof_5_16	30.0	32.0	0.1875	0.1875	0.2500	0.3125	2.0	0.1875	31.0	32057	1.635

Table 5-13: Results for roof thickness study

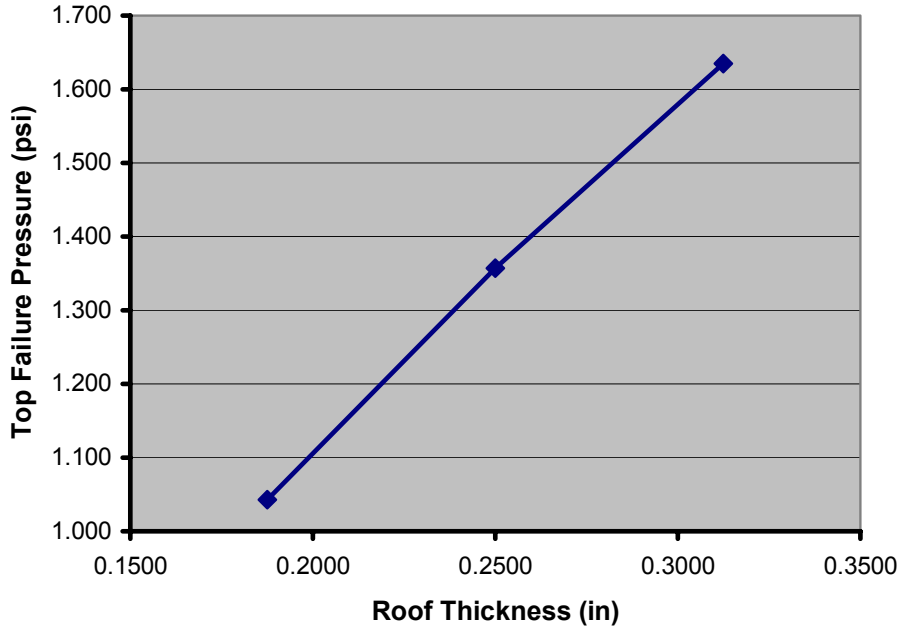

Figure 5-5: Plot of roof thickness results

5.2.4 Roof Attachment Study

Results for the roof attachment study are given in Table 5-14. The orientation of the angle at the roof attachment did not significantly change the results. However, overlapping the angle with the shell did increase the roof-to-shell joint failure pressure by approximately 9%.

Case	Dia (ft)	Height (ft)	Bottom Course (in)	Top Course (in)	Floor Thick (in)	Roof Thick (in)	Angle Width (in)	Angle Thick (in)	Angle Orient	Angle Overlap	Liquid Level (ft)	Weight (lb)	Top Failure (psi)
Attach-1	30.0	32.0	0.1875	0.1875	0.2500	0.1875	2.0	0.1875	out	no	31.0	28435	1.043
Attach-2	30.0	32.0	0.1875	0.1875	0.2500	0.1875	2.0	0.1875	in	no	31.0	28316	1.044
Attach-3	30.0	32.0	0.1875	0.1875	0.2500	0.1875	2.0	0.1875	out	yes	31.0	28532	1.124
Attach-4	30.0	32.0	0.1875	0.1875	0.2500	0.1875	2.0	0.1875	in	yes	31.0	32057	1.133

Table 5-14: Results for roof attachment study

5.2.5 Bottom Thickness Study

Results for the bottom thickness study are given in Table 5-15 and Figure 5-6.

Case	Dia (ft)	Height (ft)	Bottom Course (in)	Top Course (in)	Floor Thick (in)	Roof Thick (in)	Angle Width (in)	Angle Thick (in)	Liquid Level (ft)	Weight (lb)	Bottom Failure (psi)
floor_1_8.a	30.0	32.0	0.1875	0.1875	0.1250	0.1875	2.0	0.1875	0.0	28435	0.801
floor_1_8.b	30.0	32.0	0.1875	0.1875	0.1250	0.1875	2.0	0.1875	16.0	28435	1.863
floor_1_8.c	30.0	32.0	0.1875	0.1875	0.1250	0.1875	2.0	0.1875	31.0	28435	2.559
floor_2_8.a	30.0	32.0	0.1875	0.1875	0.2500	0.1875	2.0	0.1875	0.0	28435	1.270
floor_2_8.b	30.0	32.0	0.1875	0.1875	0.2500	0.1875	2.0	0.1875	16.0	28435	2.437
floor_2_8.c	30.0	32.0	0.1875	0.1875	0.2500	0.1875	2.0	0.1875	31.0	28435	3.265
floor_3_8.a	30.0	32.0	0.1875	0.1875	0.3750	0.1875	2.0	0.1875	0.0	28435	1.441
floor_3_8.b	30.0	32.0	0.1875	0.1875	0.3750	0.1875	2.0	0.1875	16.0	28435	2.735
floor_3_8.c	30.0	32.0	0.1875	0.1875	0.3750	0.1875	2.0	0.1875	31.0	28435	3.691

Table 5-15: Results for the bottom thickness study

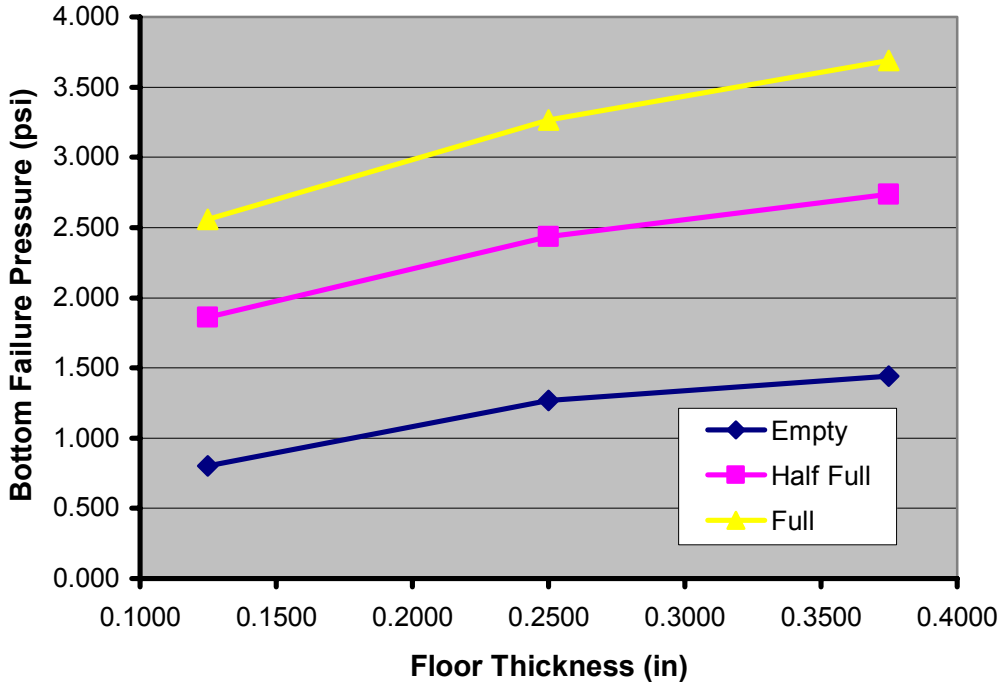

Figure 5-6: Plot of results for floor thickness study

5.2.6 Yield Stress Variation Study

For all of the other calculations reported, the minimum yield strength was assumed to be 36 ksi. This study looked at the effect of other yield strengths.

Case	Dia (ft)	Height (ft)	Bottom Course (in)	Top Course (in)	Floor Thick (in)	Roof Thick (in)	Angle Width (in)	Angle Thick (in)	Liquid Level (ft)	Weight (lb)	Yield Stress ksi)	Top Failure (psi)	Bottom Failure (psi)
ys_36.a	30.0	32.0	0.1875	0.1875	0.2500	0.1875	2.0	0.1875	0.0	28435	36	1.043	1.270
ys_36.b	30.0	32.0	0.1875	0.1875	0.2500	0.1875	2.0	0.1875	16.0	28435	36	1.043	2.437
ys_36.c	30.0	32.0	0.1875	0.1875	0.2500	0.1875	2.0	0.1875	31.0	28435	36	1.043	3.255
ys_48.a	30.0	32.0	0.1875	0.1875	0.2500	0.1875	2.0	0.1875	0.0	28435	48	1.450	1.681
ys_48.b	30.0	32.0	0.1875	0.1875	0.2500	0.1875	2.0	0.1875	16.0	28435	48	1.441	2.907
ys_48.c	30.0	32.0	0.1875	0.1875	0.2500	0.1875	2.0	0.1875	31.0	28435	48	1.442	3.760
ys_60.a	30.0	32.0	0.1875	0.1875	0.2500	0.1875	2.0	0.1875	0.0	28435	60	1.880	2.138
ys_60.b	30.0	32.0	0.1875	0.1875	0.2500	0.1875	2.0	0.1875	16.0	28435	60	1.880	3.407
ys_60.c	30.0	32.0	0.1875	0.1875	0.2500	0.1875	2.0	0.1875	31.0	28435	60	1.879	4.303

Table 5-16: Results for the yield strength variation study

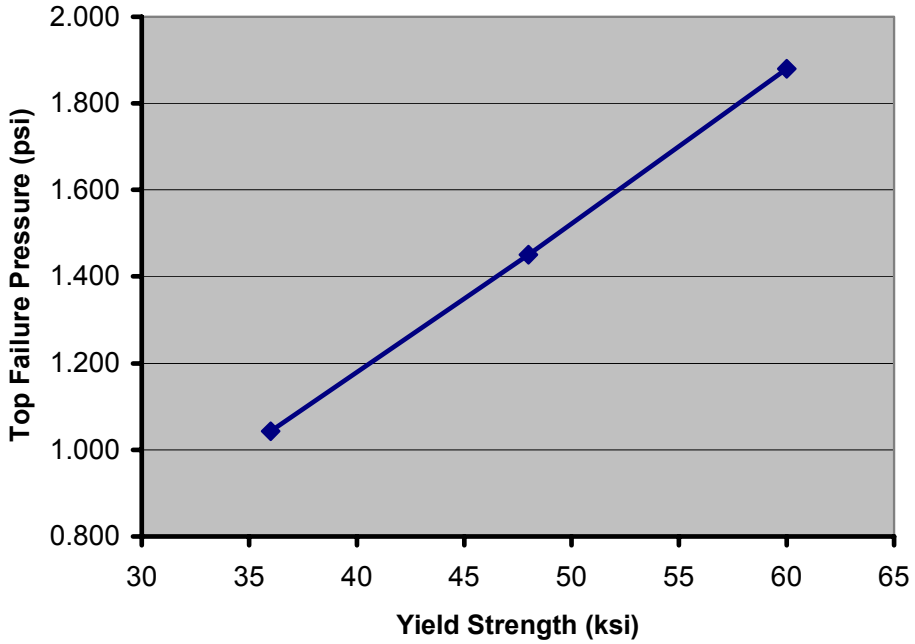

Figure 5-7: Plot showing dependence of top failure on material yield strength

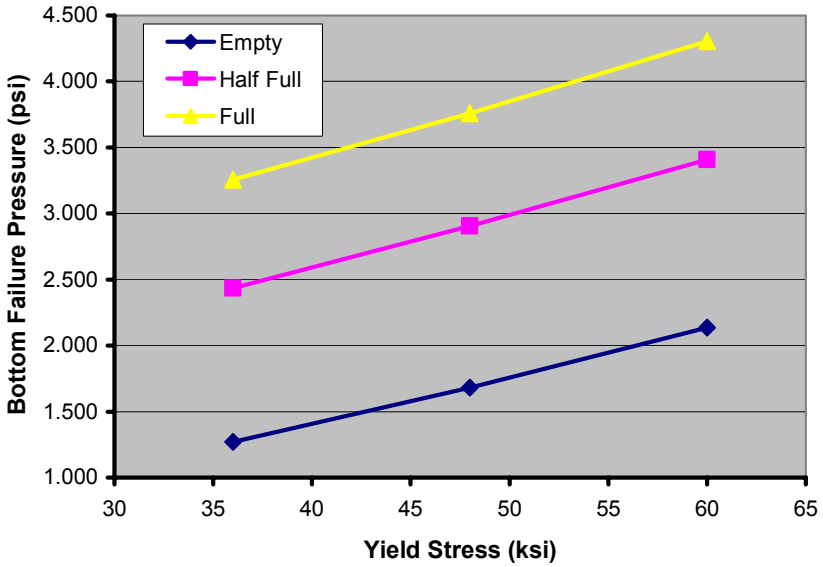

Figure 5-8: Bottom failure pressure as a function of yield stress

5.3 Dynamic Elastic-Plastic Calculations

As part of this project, dynamic, large displacement, elastic-plastic analysis capability was added to SafeRoof. This was accomplished using the FMA-3D code (Key, 2004). The following description of FMA-3D is taken from the Theoretical Manual.

> "The program is designed to compute the time-dependent displacements, velocities, accelerations, and stresses within elastic or inelastic, three-dimensional bodies composed of arbitrary shapes and materials. The program is a candidate for use in applications either where large energies and forces are present, where stress wave propagation is occurring, or where large displacements and strains dominate. Applications characterized by small forces and in¯nitesimal strains are not precluded, however. Applications for which the programs of this class have seen use fall into the areas of spent nuclear fuel shipping cask impact studies, explosive and high-rate metal forming, structures subjected to internal or external blast, and buried structure survivability studies.
>
> An accident is a typical situation requiring the analysis of a structure's transient dynamic response. Virtually every industry is faced with the problem of accidents, either in terms of the plants and facilities it operates or the products it designs. Accident analyses focus on the worst case, the unexpected, and the disabling situation. It is not the normal operating loads which are considered, but rather the extreme loads to which a structure is to be subjected. The structure may no longer be useful for its original purpose, but it should not become part of a chain of events leading to damage beyond that from the original stimulus. In these cases, it is the large deformation, the sudden dynamic excursions, and the inelastic material behavior that need to be modeled."

FMA-3D is distributed freely under the GNU license. To meet GNU license requirements and still incorporate FMA-3D with SafeRoof, the approach taken was to modify SafeRoof so that the user can select either a static analysis or a dynamic analysis. If a static analysis is requested, then the internal SafeRoof solution is used. If a dynamic analysis is requested, an input file for FMA-3D is written and the FMA-3D calculation automatically started. At the end of the FMA-3D analysis, the results are read from the FMA-3D output files and plotted in SafeRoof. By taking this approach, it was not necessary to make changes to FMA-3D, while, to the user, the FMA-3D analysis appears seamlessly integrated.

FMA-3D is implemented only as a 3D program, with no 2D axisymmetric elements. The element used for the analysis was a 4-node plate element (P4EL), Figure 5-9. The 3D model represented a 5 degree slice of the tank, with appropriate symmetry boundary conditions so that the response was axisymmetric. All material properties were assigned from the SafeRoof input data. The internal load of product in the tank is represented by a linearly increasing pressure with depth. This does not include any mass effects due to the product, which would only serve to further slow uplift and bottom joint failure and thus is conservative.

The FMA-3D model uses contact elements under the tank floor to represent the deformation and uplift. At the roof, rafter support is also modeled using contact elements.

The FMA-3D calculation is actually performed in two stages. In the first calculation, all static loads including gravity and product loads are applied to the model. A dynamic relaxation run is

then performed, where damping is included in the analysis and the dynamic analysis is continued until static equilibrium is reached. This gives a static solution in which the tank has settled on its foundation and the roof is being supported by rafters. The static equilibrium state is then used as the initial condition for the transient analysis in which the internal pressure loads are added.

The user has the option of specifying a linear ramp pressure loading on the tank or using the SafeRoof combustion capability to calculate the pressure load. The linear ramp can be used to specify such a slow ramp that the tank response is essentially static.

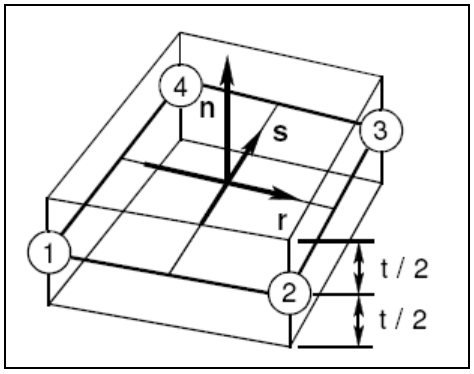

Figure 5-9: 4-node plate element (FMA, 2004)

During post-processing, displacements at the floor and elements at the top and bottom joints are monitored to identify the onset of yielding and uplift. The time steps at which yielding occurred are then available for plotting.

5.3.1 Slow Ramp Analyses using FMA-3D

Calculations were performed using the FMA-3D dynamic analysis capability to first verify the static SafeRoof calculations. To do this, a linear ramp pressure load was applied over 20 seconds. The maximum pressures were 2, 3, and 4 psi for the empty, half full, and full cases respectively. The pressures were chosen based on expected failure pressures and the ramp time was estimated both using the frequencies of the tank and trials to ensure minimal dynamic effects.

Results are presented in Table 5-17 and Table 5-18. As can be seen, the slow ramp results are consistent with the previously calculated static results. The difference in failure pressures between the slow ramp and results calculated using the SafeRoof static analysis are in nearly all cases less than 10%. One case, failure at the bottom joint for an empty tank shows larger differences (16.5%). Perhaps this case could be re-run with an even slower ramp. The good comparison with results validates the previous static analyses performed using SafeRoof. This gives high confidence in both the static, large displacement elastic SafeRoof analysis and the dynamic, large displacement, elastic-plastic FMA-3D model.

Case	Dia (ft)	Height (ft)	Liquid Level (ft)	First Uplift (psi)			Top Joint Failure								
							Ptop (psi)			Uplift R (in)			Uplift (in)		
				Dyn	Static	%	Dyn	Static	%	Dyn	Static	%	Dyn	Static	%
4.a	30.0	32.0	0.0	0.320	0.295	8.5%	1.120	1.040	7.7%	98.0	98.0	0.0%	4.230	4.684	-9.7%
4.b	30.0	32.0	16.0	0.600	0.560	7.1%	1.140	1.045	9.1%	169.5	170.5	-0.6%	0.271	0.185	46.5%
4.c	30.0	32.0	31.0	0.880	0.804	9.5%	1.120	1.046	7.1%	176.3	176.3	0.0%	0.034	0.027	25.9%

Table 5-17: Results of slow ramp analysis for top joint failure

Case	Dia (ft)	Height (ft)	Liquid Level (ft)	First Uplift (psi)			Bottom Joint Failure								
							Pbot (psi)			Uplift R (in)			Uplift (in)		
				Dyn	Static	%	Dyn	Static	%	Dyn	Static	%	Dyn	Static	%
4.a	30.0	32.0	0.0	0.320	0.295	8.5%	1.480	1.270	16.5%	86.0	90.0	-4.4%	5.292	5.512	-4.0%
4.b	30.0	32.0	16.0	0.600	0.560	7.1%	2.400	2.437	-1.5%	155.0	153.0	1.3%	2.841	2.758	3.0%
4.c	30.0	32.0	31.0	0.880	0.804	9.5%	3.040	3.255	-6.6%	161.0	161.0	0.0%	2.441	2.346	4.0%

Table 5-18: Results for slow ramp for bottom joint failure

5.3.2 Combustion Analyses using FMA-3D

Dynamic analyses were also performed using the combustion option in SafeRoof. These analyses were done for empty, half full, and full tanks. The ignition point was assumed to be in the center of the available free space.

The combustion pressures are shown in Figure 5-10 and Figure 5-11. The combustion calculations were continued up until pressures of approximately 100 psi, Figure 5-10. Of more interest are the early pressures shown in Figure 5-11. As can be seen, the full tank has the highest rate of pressure increase, while the empty tank has the slowest. The reason is that the available volume for expansion of the combustion is much smaller in the full tank.

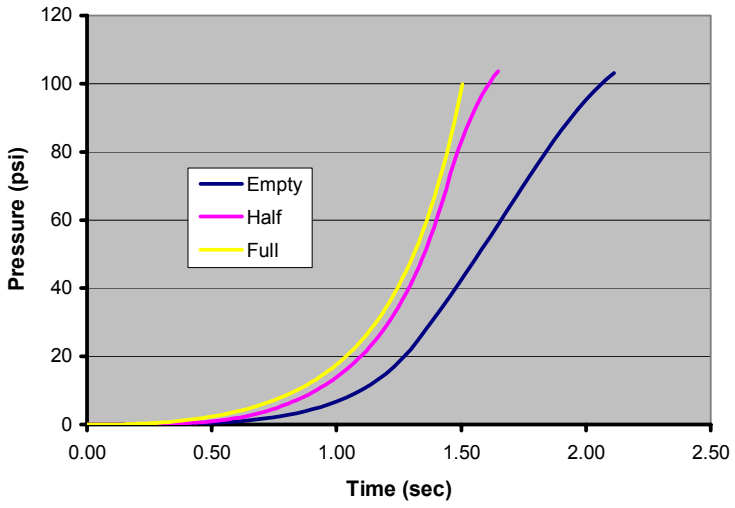

Figure 5-10: Combustion pressure in tank

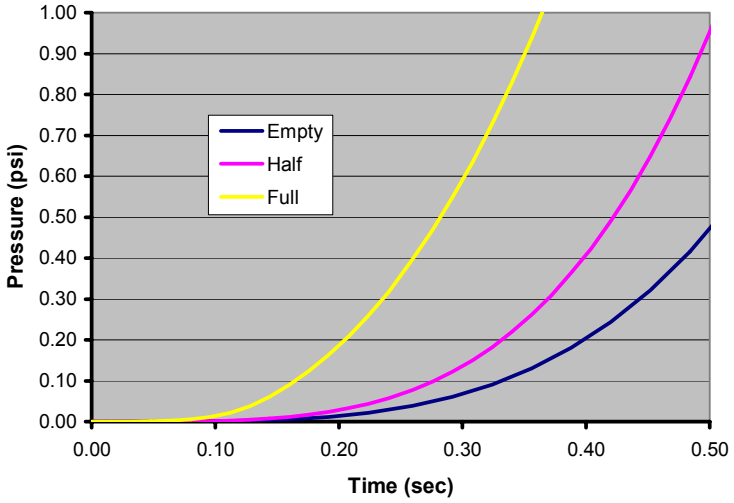

Figure 5-11: Detail of combustion pressures showing first 0.5 sec

These combustion time histories were then used in the dynamic analysis (this is done automatically in the new SafeRoof). Results are shown in Table 5-19. The pressures at failure are somewhat larger than for the static cases, but are quite close. In all cases, dynamic effects serve to delay failure.

This can be seen by looking at the top joint failure pressures in the dynamic case. For static analyses, the top joint failure is independent of the product level in the tank and is approximately 1.045 psi. For the dynamic combustions analyses, top joint failure occurs at a pressure of 1.191 psi for an empty tank and 1.310 psi for a full tank. This corresponds to the more rapid loading of the full tank. In the dynamic analysis, the mass of the tank slows deformation so that a higher pressure is reached at tank failure. The tank is not stronger, there is just a lag between the loading and the deformation of the tank.

In only one case does the dynamic, elastic-plastic calculation give a lower failure pressure than the static elastic analysis. This is for the pressure to cause bottom joint failure for the full tank. For a full tank, there is considerable bending occurring at the bottom joint before failure. Middle surface (membrane) yielding is used as the failure criteria for the joint. However, because the elastic-plastic analysis includes yielding at the inner and outer surfaces, this reduces the moment carried before failure and likely is the cause of the lower pressure for failure.

The general rule is that including dynamic effects delays failure. Including an elastic-plastic analysis can reduce failure pressure in specific cases, but the difference from the elastic, large displacement, static analyses is still relatively small. If the inertia of the product was included in the analyses, this would likely delay failure further.

Case	Dia (ft)	Height (ft)	Liquid Level (ft)	First Uplift (psi)		Top Joint Failure						Bottom Joint Failure					
						Ptop (psi)		Uplift R (in)		Uplift (in)		Pbot (psi)		Uplift R (in)		Uplift (in)	
				Dyn	Static	Dyn	Static	Dyn	Static	Dyn	Static	Dyn	Static	Dyn	Static	Dyn	Static
4.a	30.0	32.0	0.0	0.356	0.295	1.191	1.040	118.0	98.0	3.170	4.684	1.530	1.270	90.0	90.0	5.240	5.512
4.b	30.0	32.0	16.0	0.595	0.560	1.222	1.045	171.5	170.5	0.159	0.185	2.815	2.437	153.0	153.0	3.376	2.758
4.c	30.0	32.0	31.0	0.916	0.804	1.310	1.046	175.8	176.3	0.039	0.027	3.077	3.255	161.0	161.0	2.415	2.346

Table 5-19: Results of dynamic combustion analyses

5.4 Discussion of Results

Several general observations can be made of tank behavior:

1. The amount of uplift, especially for empty tanks, can be significant. The maximum at the roof-to-shell joint failure pressure is approximately 5 inches. For large tanks with diameters over 100 feet, there may not be any uplift at the top joint failure pressure. This is because the large tanks are heavier and the top joint failure pressures for large tanks are lower.
2. For full tanks, the pressure required to fail the bottom joint is larger than when empty. As a result, full tanks have a larger margin between the pressure required to fail the bottom joint and the pressure required to fail the top joint.
3. As the slope of the roof increases, the strength of the roof-to-shell joint increases significantly.
4. The static, large deformation, elastic analysis results are in good agreement with slow ramp loading calculations using a dynamic, large deformation, elastic-plastic analysis.
5. Some dynamic effects are noted in the top failure during the combustion analysis, but since dynamic effects serve to delay failure, the consequence is that using static calculations is conservative for design.
6. Buckling reduces the failure pressures for the top and bottom joints. Results have been presented with and without buckling. These results provide bounds on the expected failure pressures.

These observations will impact the suggested design criteria.

6. Proposed Design Criteria

The analyses indicate the following significant points applicable to tanks that are intended to have a frangible roof-to-shell joint:

1. For smaller tanks, significant uplift can be expected to occur at the top joint failure pressure. This means that the simple criterion of no uplift can not be used in the API 650 standard.
2. For all tanks, the bottom joint failure pressure increases when the tank is full. This essentially means that the bottom joint is stronger when the tank is full. The reason for this behavior is that higher pressures are needed to uplift a full tank than an empty tank.
3. For some larger tanks, no uplift is expected. For these tanks, no additional evaluation is required. Also, if the tank is anchored so that minimal uplift will occur, then the shell-to-bottom joint should be protected and not additional evaluation required.
4. For tanks expected to experience uplift, it is suggested that the design criteria be based on the relative strength of the bottom joint to the top joint. For empty tanks the suggested joint failure ratio is 1.5 and for full tanks the suggested joint failure ratio is 2.5 (joint failure ratio is the pressure to fail the shell-to-bottom joint divided by the pressure to fail the roof-to-shell joint). The reduced margin for empty tanks is based on an assumption that empty tanks represent a smaller safety hazard.
5. For tanks expected to experience uplift, it is necessary to ensure adequate strength in the bottoms of the tanks. This can be accomplished in two ways: (1) demonstrating that the stresses in the bottom are below the allowable, or (2) requiring full penetration butt welded bottom plates for a radial width from the shell of $[(R - R_{up}) + 24]$ inches.

Based on the analyses performed and the above observations, the rules in Figure 6-1 and Figure 6-2 are suggested as one approach that API might take to ensure frangibility of all tanks. Figure 6-1 gives the rules for an empty tank, while Figure 6-2 gives rules for a full tank. It is necessary for the designer to check both empty and full tanks.

These suggested rules take into account the relative danger of empty vs. full tanks, by using different safety margins and different allowable uplift displacements for empty and full tanks. Appendix A provides equations for calculation of all of the design parameters.

The steps for an empty tank are as follows:

1. Calculate the basic parameters for the analysis – the pressure to cause failure at the roof-to-shell joint, $P_{top\ fail}$, the pressure to cause failure of the shell-to-bottom joint, $P_{bot\ fail}^{empty}$, the pressure at 1.5 times the pressure to fail the roof-to-shell joint, $P_{\text{margin}}^{1.5} = 1.5 * P_{top\ fail}$, and the uplift pressure, P_{uplift}^{empty}. Our goal is to make sure that the tank is safe at a pressure 1.5 times the pressure to fail the roof-to-shell joint.
2. Check to see if uplift will occur at a pressure of $P_{\text{margin}}^{1.5}$. If not, then the bottom stresses will be low and we do not need to do any further calculations. Larger tanks will fall into this category.

3. If uplift will occur, verify that $P_{\text{margin}}^{1.5}$ is less than the pressure to fail the tank bottom. If it is not, then the tank must be redesigned to provide a larger margin of strength. If this test is passed, then continue the following calculations using $P_{\text{margin}}^{1.5}$.
4. Calculate the allowable stress for the bottom welds, σ_{allow}^{bot}, and the uplift radius, $R_{up}^{1.5}$. The allowable stress is based on the weld strength. The uplift radius is the radius at which the bottom begins to uplift from the foundation.
5. If the tangential stress in the bottom is less than the allowable, proceed with the calculation. Otherwise, it is necessary to either modify the design or to specify full penetration butt welds for the bottom plates from the shell-to-bottom joint to a radius of $R_{up}^{1.5} - 24$ inches.
6. Calculate the uplift, $D_{up}^{1.5}$, at the 1.5 pressure. This is the uplift of the shell from the foundation.
7. Verify that all attachments can accommodate an uplift of $D_{up}^{1.5}$. If they can not, the attachments will need to be redesigned.
8. If all the steps have been passed successfully, the design calculation for the empty condition is finished. Next proceed to repeat these calculations for a full tank.

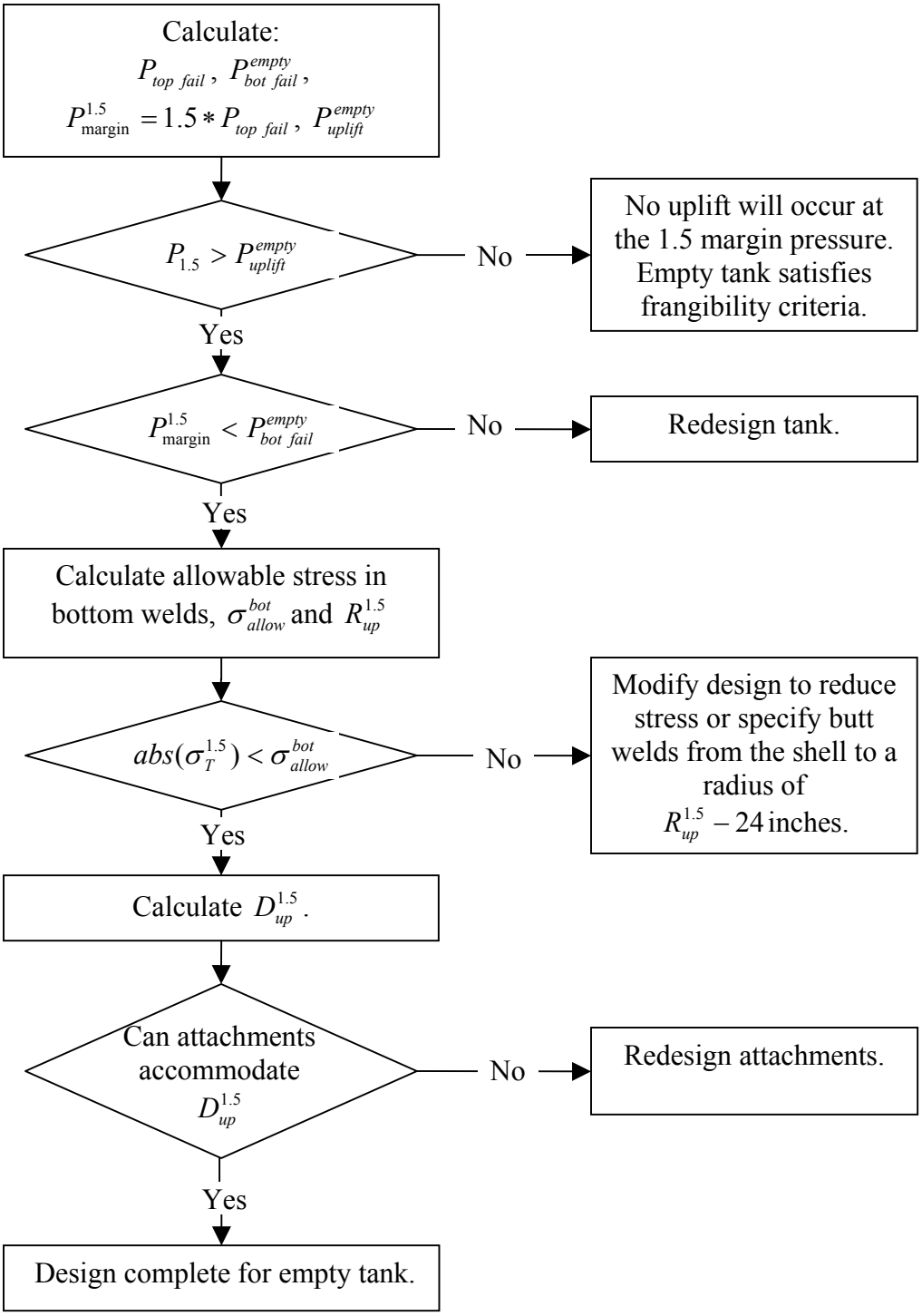

Figure 6-1: Suggested design flow for empty frangible roof tanks (both empty and full criteria must be met).

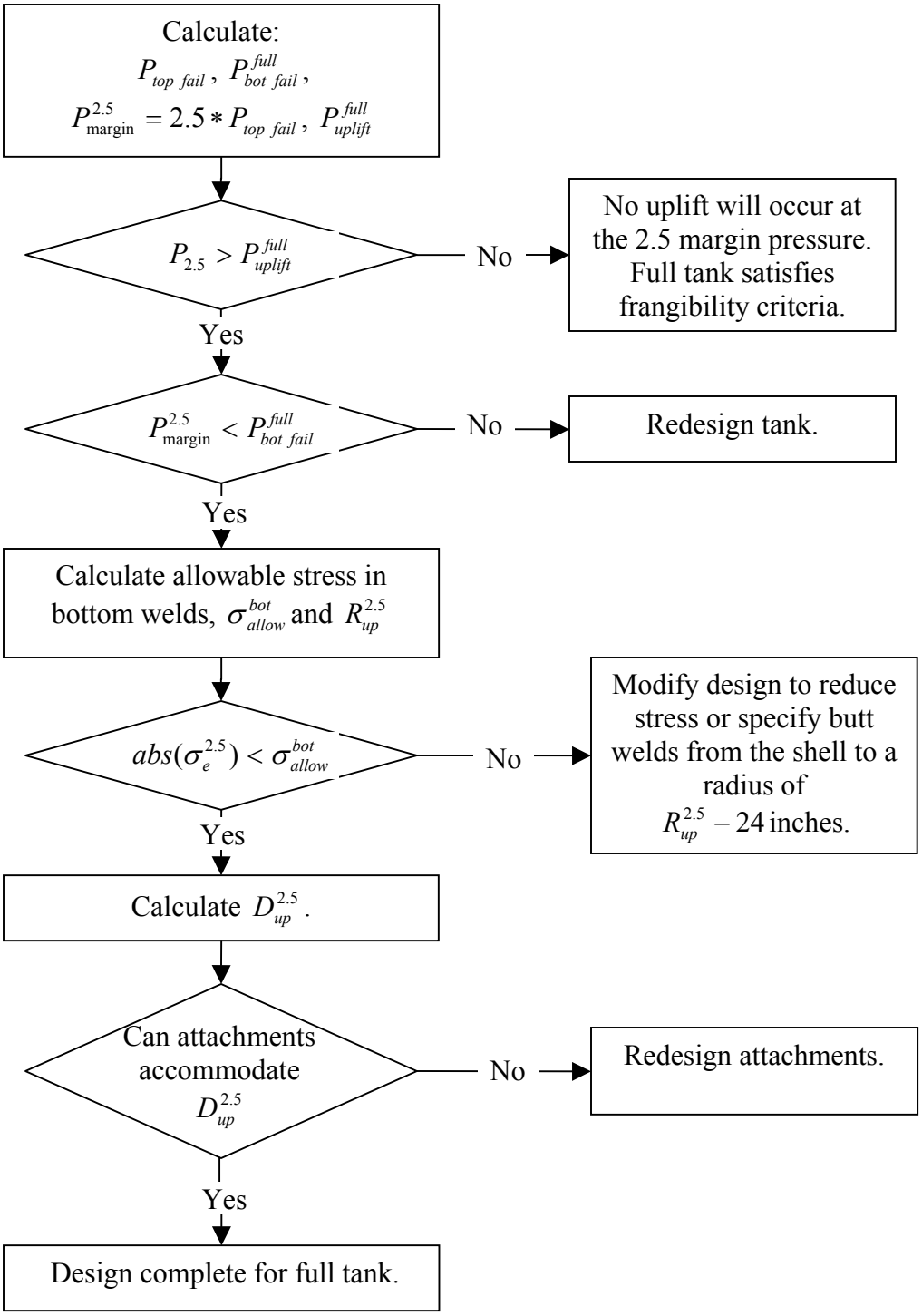

Figure 6-2: Suggested design flow for full frangible roof tanks (both empty and full criteria must be met)

7. Design Changes that Enable Small Tanks to Meet New Criteria

Large tanks often satisfy the new design criteria with no changes. However, smaller tanks may require some design changes if they are to satisfy the frangibility criteria. Usually just making the bottom course thicker will result in the desired strength margin for the joint failure pressures. Of course, it will also be necessary to ensure that full-penetration butt welds are used in much of the bottom and that the attachments can meet the calculated uplift.

As an example, we use the Case 1 tank with a 0.75 inch slope. In the original design, the thickness of the bottom course was 0.1875 inches, this gave a strength ratio of 1.06 when empty and 2.0 when full. By changing the bottom course to a thickness of 0.375 inches, the strength ratio becomes 1.5 empty and 2.9 when full. Alternately, increasing the bottom thickness to 0.3125 inches and a bottom course thickness of 0.25 inches gives an empty strength ratio of 1.5 and a full strength ratio of 2.6. Either of these approaches gives an adequate strength ratio.

For the case with 0.375 inch thickness of the bottom course at 1.5 times the top joint failure pressure ($P_{1.5}$), the empty uplift is 4.4 inches with an uplift radius of 46 inches. For the second case, the empty uplift is also 4.4 inches and the uplift radius is 42 inches. This means that the bottom would need to be butt-welded over nearly all its extent and attachments would need to be designed to accommodate approximately 4.5 inches of vertical tank displacement. Possibly piping could be attached at the center of the bottom to avoid uplift altogether.

8. Miscellaneous Items for Consideration

The following points are mentioned for consideration by the committee:

1. It is assumed that empty tanks are a smaller safety problem than full tanks. However, this is not based on data. Is this assumption correct?
2. Since the product level in the tank increases the pressure required to fail the shell-to-bottom joint, one approach could be to require a minimum product level for frangibility of existing tanks.
3. The effect of buckling reduces the joint failure pressures and gives a range for expected failures.
4. Base on the linearization of the results in the log-log plots, this might provide a different approach to defining simplified design equations for failure pressure.

9. Conclusions

This report has investigated the failure of smaller tanks in which uplift can occur. This uplift makes it necessary to develop new criteria to ensure that the failure pressure of the roof-to-shell joint is less than the shell-to-bottom joint. The criteria must accommodate the uplift that occurs in smaller tanks. The criteria establish:

1. Strength ratios that must be satisfied for the strength of the roof-to-shell joint as compared to the shell-to-bottom joint.
2. Changes in bottom design that are necessary to ensure that the bottom does not fail in the event of uplift.
3. Changes in the design of attachments that must now accommodate the expected uplift.
4. Results show that dynamic effects are relatively small and that they serve to delay failure. Therefore, use of static analysis is conservative.

If these criteria are adopted by the API 650 committee, it is possible to design small tanks that meet these criteria. Most larger tanks already meet the criteria, although it will be necessary to ensure that attachments can accommodate uplift for some intermediate size tanks.

10. References

API Standard 650, "Welded Steel Tanks for Oil Storage," Tenth Edition, November 1998, Addendum 1, January 2000, and Addendum 2, November 2001.

FMA, "FMA-3D User's Guide," Code and Documentation by Samuel Key, FMA Development, LLC, 1851 Tramway Terrace Loop NE, Albuquerque, New Mexico, 87122, (505) 856-1588, Version 20.00, August, 2003.

Juvinall, Robert, and Marshek, Kurt, *Fundamentals of Machine Component Design*, John Wiley & Sons, Inc., 3rd Edition, 2000.

Lu, Zhi, and Swenson, Daniel, 1994, "User's Manual for SafeRoof: A Program for the Analysis of Storage Tanks with Frangible Roof Joints," Manual Release 1.0, Mechanical Engineering Dept., Kansas State University, Manhattan, KS, 66506.

Morgenegg, E. E., 1978, "Frangible Roof Tanks," Proceedings Am. Pet. Inst. Refin. Dep., Midyear Meet., 43rd, Toronto, Ont., May 8-11, 1978, Pub. By API (v57), Washington, DC, p. 509-514.

Swenson, Daniel; Fenton, Don; Lu, Zhi; Ghori, Asif; and Baalman; Joe, "Evaluation of Design Criteria for Storage Tanks with Frangible Roof Joints," Welding Research Council Bulletin 410, ISSN 0043-2326, Welding Research Council, United Engineering Center, 345 East 47th Street, New York, NY, 10017, April, 1996.

11. Acknowledgements

We thank George Morovich, Phillip Myers, Rob Ferry, and Larry Hiner for comments and suggestions on this work. This effort was funded by the American Petroleum Institute.

We also thank Sam Key for providing the FMA-3D code, which he has developed based on his lifetime experience in large deformation analysis and distributes through the free GNU license. We also thank him for his help in answering questions on the use of FMA-3D.

A. Appendix: Simplified Design Calculations

Note: Because the linearization of the results in the log-log plots appears that it might provide an improved approach to developing design equations, the design equation coefficients calculated using the previous draft report were not updated in this report to include the effect of buckling or the corrected angle sizes in the designs. The equations are still essentially consistent with the calculations, but it is recommended that a different approach be explored for derivation of these approximating equations.

This section describes the simplified analyses that can be used by designers to ensure their designs meet the frangible roof-to-shell joint criteria.

A.1 Effective Stress

The "effective stress" defines the yield surface in 3D space. It provides a way to compare a 3D stress state to a yield stress. Other names for this yield theory include "von Mises" or "Maximum Distortion Energy" (Juvinall and Marshek, 2000).

In terms of principal stresses, the equivalent stress (σ_e) is:

$$\sigma_e = \frac{\sqrt{2}}{2}\left[(\sigma_2 - \sigma_1)^2 + (\sigma_3 - \sigma_1)^2 + (\sigma_3 - \sigma_2)^2\right]^{1/2} \quad \text{Eqn. 1}$$

For an axisymmetric shell, we assume the shear stresses and through-thickness stresses are small. Then this reduces to:

$$\sigma_e = \frac{\sqrt{2}}{2}\left[(\sigma_r)^2 + (\sigma_\theta - \sigma_r)^2 + (\sigma_\theta)^2\right]^{1/2} \quad \text{Eqn. 2}$$

In the case of a single shear stress, the equivalent stress is given by:

$$\sigma_e = \sqrt{3}\tau \quad \text{Eqn. 3}$$

A.2 Uplift Pressure

A.1.1 Empty Tank

The uplift pressure is the pressure that first causes uplift of the tank at the radius of the shell. It is calculated by simple equilibrium between the upward pressure on the tank roof and the weight (W) of the tank roof, shell, and attachments (bottom not included). This gives:

$$P_{uplift} = \frac{W}{\pi R^2} \quad \text{Eqn. 4}$$

A.1.2 Full Tank

For a full tank, the pressure to first cause uplift depends on the tank design and the foundation. This equation assumes a tank on sand with a ringwall foundation, with a sand foundation stiffness of 250 psi/in and a ringwall stiffness of 1000 psi/in.

$$P_{uplift}^{rull} = 1.15 - 1.536 * 10^{-4} D^2 + 4.124 * 10^{-6} W - 1.309 * 10^{-3} * \frac{\sqrt{Dt}}{t^3} - 5.103 h_{product} \quad \text{Eqn. 5}$$

A.3 Roof-to-Shell Joint Failure Pressure

The roof to shell joint failure pressure design calculations can be performed using a modification of the present calculation for compressive area.

$$w_c = (3.41 - 9.68\sin(\theta))(R_c t_s)^{0.5} \quad \text{Eqn. 6}$$

$$w_h = (0.96 - 0.42\sin(\theta))(R_2 t_h)^{0.5} \quad \text{Eqn. 7}$$

where w_c = width of participating shell and w_h = width of participating roof. θ and R_2 are defined in API 650. The limit on w_h is removed.

These values were obtained by minimizing the square of the errors between the SafeRoof calculation of top joint failure pressure and the design calculation described above. This was performed in a spread sheet and used the Excel Solver to find the coefficients.

To calculate the new failure pressure, first calculate the compression area (A) using w_c and w_h, above. The failure pressure is then:

$$P_{fail}^{top} = \frac{2A\sigma_y Slope}{12 * R^2} \quad \text{Eqn. 8}$$

where $Slope$ is the rise per 12 inches of radius and the radius is measured in inches.

This equation has not been updated to reflect buckling or the minor changes due to angle thickness from the draft report. It is recommended that an alternate derivation be attempted using the log-log plots of the calculations.

A.4 Shell-to-Bottom Joint Failure Pressure

Failure of the shell-to-bottom joint is defined to occur when the middle (membrane) stress in the bottom of the shell reaches yielding. As described in Section 2.1, the most significant stress component is a large compressive circumferential stress. Because there can be a large moment at this joint, the maximum stress can be located 1 to 2 inches above the bottom. For the failure calculation, this maximum stress is used.

The response of the empty and full tanks is different, so equations were developed for empty and full tanks. Eqn. 9 and Eqn. 10 give the pressure at which the bottom joint fails. Unfortunately, the importance of large displacement (uplift) at this joint makes it difficult to develop a simple analysis.

$$P_{PBotEmpty} = 2.473 - 4.588 * 10^{-2} D + 1.965 * 10^{-4} D^2 - 1.067 * 10^{-6} W - 1.065 * 10^{-3} * \frac{\sqrt{Dt}}{t^3} + 1.813t$$

Eqn. 9

$$P_{PBotFull} = 2.512 - 1.574 * 10^{-2} D - 1.170 * 10^{-3} D^2 + 4.094 * 10^{-5} W + 1.557 * 10^{-3} * \frac{\sqrt{Dt}}{t^3} + 1.823t$$

Eqn. 10

These equations were obtained by defining the functions and then minimizing the square of the error with respect to the values calculated by SafeRoof. This was performed in a spread sheet and used the Excel Solver to find the coefficients.

This equation has not been updated to reflect buckling or the minor changes due to angle thickness from the draft report. It is recommended that an alternate derivation be attempted using the log-log plots of the calculations.

A.5 Uplift Radius

If the pressure exceeds the uplift pressure, then the uplift radius (the radius at which the bottom is not longer in contact with the foundation) is calculated using simple equilibrium of the tank, Figure A.5-1. We assume that the part of the bottom still resting on the foundation is in equilibrium with the internal loads downward on the tank bottom.

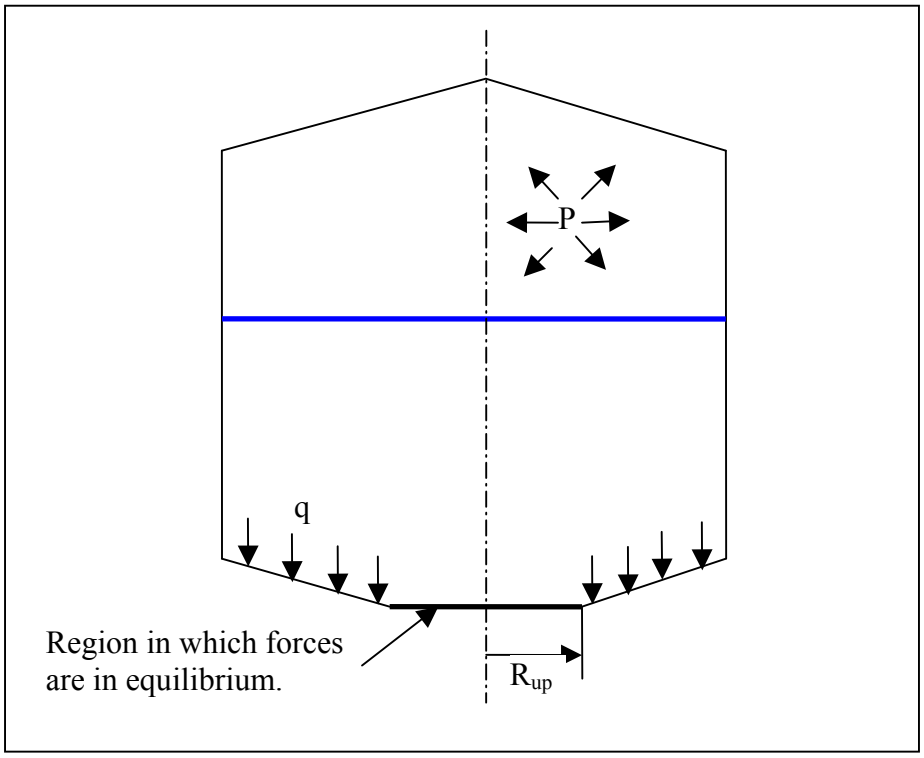

Figure A.5-1: Free body diagram of tank with uplift

Equating the upward and downward forces:

$$F_{up} - F_{down} = 0 \qquad \text{Eqn. 11}$$

or:

$$P\pi R^2 - Weight - \left(P + P_{liq} + t_{floor}\rho_{floor}\right)\pi\left(R^2 - R_{up}^2\right) = 0 \qquad \text{Eqn. 12}$$

We can write the expressions for the areas:

$$P\pi R^2 - Weight - \left(P + P_{liq} + t_{floor}\rho_{floor}\right)\pi\left(R^2 - R_{up}^2\right) = 0 \qquad \text{Eqn. 13}$$

This simplifies to:

$$R_{up} = \left[\frac{W + \left(P_{liq} + t_{floor}\rho_{floor}\right)\pi R^2}{\pi\left(P + P_{liq} + t_{floor}\rho_{floor}\right)}\right]^{1/2} \qquad \text{Eqn. 14}$$

Thus, given the internal and product pressures, the uplift of the tank can be calculated.

A.6 Uplift Displacement

Given a pressure and tank parameters, the uplift displacement of the shell can be calculated using Eqn. 15.

$$D_{Up} = 0.956 - 1.179*10^{-2}D - 1.976*10^{-4}D^2 + 1.192*10^{-5}W + 3.371*10^{-3}*\frac{\sqrt{Dt}}{t^3} +$$
$$0.993t - 4.411*10^{-2}h_{liq} - 1.164*10^{-4}h_{liq}^2 + 5.607*10^{-2}\left(R - R_{up}\right) - 4.007*10^{-5}\left(R - R_{up}\right)^2$$

Eqn. 15

This equation has not been updated to reflect buckling or the minor changes due to angle thickness from the draft report. It is recommended that an alternate derivation be attempted using the log-log plots of the calculations.

A.7 Circumferential Stress in Bottom

Given a pressure and tank parameters, the circumferential stress in the bottom at the shell-to-bottom joint are given by Eqn. 16 for empty tanks and Eqn. 17 for full tanks:

$$\sigma_T^{empty} = -4.122*10^3 + 1.126*10^2(D_{ft}) - 4.820(D_{ft})^2 + 0.222(W) + 1.813*10^{-2}t_{bot} -$$
$$6.433*10^2(t_{bot\ shell}) - 1.012*10^2(h_{liq}) + 3.341(h_{liq})^2 + 4.795*10^2\left(R - R_{up}\right) - 41.232*10^4\left(D_{up}\right)$$

Eqn. 16

$$\sigma_T^{full} = -37. - 5.920*10^1\sqrt{D_{ft}} + 5.197*10^2(D_{ft}) + 8.504*10^1\sqrt{W} - 0.290(W) - 11.65\sqrt{t_{bot\ shell}} - 103.7\sqrt{h_{liq}} - 211.3(h_{liq}) - 1663.0\left(R - R_{up}\right) - 119.8\sqrt{D_{up}} - 252.4\left(D_{up}\right) - 755.8\left(D_{up}\right)^2$$

Eqn. 17

This equation has not been updated to reflect buckling or the minor changes due to angle thickness from the draft report. It is recommended that an alternate derivation be attempted using the log-log plots of the calculations.

A.8 Bottom Lap Joint Failure Stress

The bottom plates are welded using a lap joint, Figure A8-1.

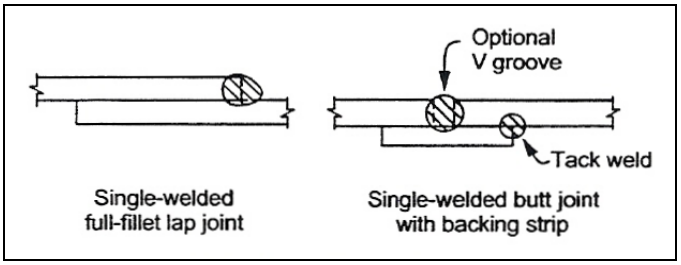

Figure A.8-1: Detail of bottom lap joints

The definition of terms for a weld are given in Figure A.8-2.

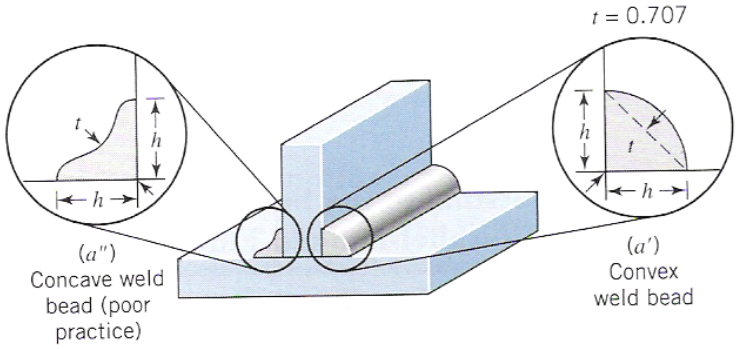

Figure A.8-2: Definition of weld parameters (Juvinall and Marshek, 2000)

A standard approach to design of a lap weld is to assume that the load is carried by shear stresses through an area defined by the throat of the weld (t in Figure A.8-1). We will assume the weld is at yield and determine the corresponding stress in the plate. The leg length of the weld is assumed to be the same as the plate thickness.

Using the equivalent stress, the shear stress to cause yield is given by:

$$\tau_y = 0.577\sigma_y \qquad \text{Eqn. 18}$$

The load in the plate is given by:

$$F = \sigma A_{plate} \quad \text{Eqn. 19}$$

which is also equal to the load carried in the weld:

$$F = \tau_y A_{weld} \quad \text{Eqn. 20}$$

where:

$$A_{weld} = 0.707(thick)(1) \quad \text{Eqn. 21}$$

Then:

$$\sigma(thick)(1) = \tau_y (0.707)(thick)(1) \quad \text{Eqn. 22}$$

Finally, using Eqn. 18,

$$\sigma = (0.707)\tau_y = (0.707)(0.577)\sigma_y$$

$$\sigma = (0.410)\sigma_y \quad \text{Eqn. 23}$$

Thus, the maximum stress the weld can sustain is 0.41 times the yield stress of the plate.

A.9 Application of Simplified Calculations

These simplified calculations are illustrated in Table A9-1, Table A9-2, Table A9-3, and Table A9-4. The equations show reasonable correlation with the finite element calculations.

Note: These tables have not been updated to reflect buckling or the minor changes due to angle thickness from the draft report. It is recommended that an alternate derivation of the equations be attempted using the log-log plots of the calculations.

Case	Design Calculations																
	First Uplift (psi)	First Uplift Error	Top Failure					Bottom Failure		P1.5 and P2.5							
			wc (in)	wh (in)	A (in^2)	Ptop (psi)	Ptop Error	Pbot (psi)	Pbot Error	P (psi)	Rup (in)	Rup Error	R-Rup (in)	Dup (in)	Dup Error	SigT (psi)	SigT Error
1.a	0.266	-1.4%	13.326	17.753	6.202	1.938	-1.0%	1.649	-19.0%	2.907	40.3	-4.0%	79.7	6.217	23.3%	-39646.568	-8.4%
1.c	0.742	9.2%	13.326	17.753	6.202	1.938	-1.0%	3.022	-21.3%	4.846	96.0	1.1%	24.0	2.435	-12.5%	-33677.342	-10.0%
2.a	0.195	1.5%	16.321	21.743	7.512	1.043	-0.3%	1.209	3.9%	1.565	72.5	-3.3%	107.5	7.728	11.6%	-44469.919	3.4%
2.c	0.611	-18.2%	16.321	21.743	7.512	1.043	0.2%	2.702	7.2%	2.608	158.0	1.9%	22.0	2.443	-13.0%	-24974.072	-5.8%
3.a	0.159	1.6%	18.846	25.107	8.616	0.673	2.9%	0.818	2.6%	1.010	110.7	-0.3%	129.3	8.857	2.4%	-48161.353	11.9%
3.c	0.468	-6.9%	18.846	25.107	8.616	0.673	2.7%	2.181	15.3%	1.683	220.1	2.4%	19.9	2.394	-9.8%	-16262.964	-11.9%
4.a	0.279	5.3%	16.321	21.743	7.512	1.043	-0.3%	1.201	-5.5%	1.565	83.2	2.8%	96.8	7.264	13.7%	-41980.608	5.0%
4.c	0.641	20.3%	16.321	21.743	7.512	1.043	0.3%	3.054	-6.2%	2.608	165.9	1.4%	14.1	1.502	4.6%	-11538.939	19.8%
5.a	0.230	1.8%	18.846	25.107	8.616	0.673	3.1%	1.004	3.8%	1.010	126.5	2.8%	113.5	7.776	1.2%	-39607.935	6.5%
5.c	0.689	2.5%	18.846	25.107	8.616	0.673	2.6%	2.551	-6.2%	1.683	227.7	1.0%	12.3	1.086	17.9%	-3265.927	4.0%
6.a	0.234	1.7%	24.330	28.070	11.846	0.592	-3.0%	0.812	-1.1%	0.888	169.0	-1.2%	131.0	8.448	-6.4%	-37266.114	-0.9%
6.c	0.725	-5.9%	24.330	28.070	11.846	0.592	-2.6%	2.316	-4.6%	1.481	286.6	0.4%	13.4	0.968	9.8%	-2200.794	5.3%
7.a	0.286	5.3%	18.846	25.107	8.616	0.673	2.9%	1.136	2.8%	1.010	137.8	2.1%	102.2	7.059	2.0%	-33972.595	4.0%
7.c	0.831	8.7%	18.846	25.107	8.616	0.673	3.1%	2.900	-14.0%	1.683	230.4	0.0%	9.6	0.376	-4.4%	-422.212	3.0%
8.a	0.285	5.5%	24.330	28.070	11.846	0.592	-3.0%	0.916	1.6%	0.888	182.5	-0.3%	117.5	7.746	-4.3%	-31934.323	-3.4%
8.c	0.856	1.1%	24.330	28.070	11.846	0.592	-2.8%	2.869	-2.9%	1.481	289.6	-0.3%	10.4	0.350	3.0%	-61.613	-12.0%
9.a	0.255	1.8%	26.652	30.749	12.928	0.449	0.2%	0.733	-0.7%	0.673	238.2	0.5%	121.8	7.849	-10.0%	-30117.248	-1.1%
9.c	0.819	-3.7%	26.652	30.749	12.928	0.449	0.2%	2.401	-8.7%	1.122	350.8	-0.2%	9.2	0.177	0.2%	3723.195	0.0%
10.a	0.311	5.6%	26.652	30.749	12.928	0.449	0.2%	0.879	5.4%	0.673	257.9	1.1%	102.1	6.950	-4.6%	-23455.918	-3.6%
10.c	0.977	-2.8%	26.652	30.749	12.928	0.449	0.2%	3.371	7.7%	1.122	352.8	-0.7%	7.2	-0.281	0.0%		0.0%
11.a	0.275	5.4%	30.775	35.506	15.101	0.295	6.4%	0.636	-1.8%	0.442	394.0	5.1%	86.0	6.177	-13.0%	-16855.945	-5.6%
11.c	0.885	-9.0%	30.775	35.506	15.101	0.295	6.4%	2.866	12.8%	0.737	474.5	-0.3%	5.5	-0.338	0.0%		0.0%
12.a	0.256	1.9%	34.407	39.697	16.795	0.210	12.9%	0.517	-5.8%	0.315	552.2	8.3%	47.8	4.332	-23.0%	-7509.407	-26.7%
12.c	0.728	-5.0%	34.407	39.697	16.795	0.210	12.9%	2.181	0.2%	0.525	595.9	0.0%	4.1	-0.284	0.0%		0.0%
13.a	0.253	2.0%	42.140	43.486	22.260	0.193	8.9%	0.515	3.2%	0.290	681.9	6.2%	38.1	4.143	0.1%	-1693.065	-68.0%
13.c	0.569	10.4%	42.140	43.486	22.260	0.193	8.4%	1.868	-3.2%	0.483	715.8	0.1%	4.2	0.050	0.0%		0.0%

Table A9-1: Results using simplified design calculations (0.75 inch slope)

Tank Data									Design Calculations						
Case	Dia (ft)	Height (ft)	Liquid Level (ft)	Weight (lb)	Bottom Course (in)	Top Course (in)	Angle Width (in)	Angle Thick (in)	First Uplift (psi)	First Uplift Error	Top Failure				
											wc (in)	wh (in)	A (in^2)	Ptop (psi)	Ptop Error
101.a	20.0	20.0	0.0	12111	0.1875	0.1875	2.0	0.1875	0.268	0.8%	12.375	15.247	5.554	2.314	-10.2%
101.c	20.0	20.0	19.0	12111	0.1875	0.1875	2.0	0.1875	---	---	12.375	15.247	5.554	2.314	-9.3%
102.a	30.0	20.0	0.0	20009	0.1875	0.1875	2.0	0.1875	0.197	0.7%	15.156	18.673	6.718	1.244	-8.9%
102.c	30.0	20.0	19.0	20009	0.1875	0.1875	2.0	0.1875	---	---	15.156	18.673	6.718	1.244	-8.7%
103.a	40.0	20.0	0.0	29135	0.1875	0.1875	2.0	0.1875	0.161	0.6%	17.501	21.562	7.699	0.802	-6.1%
103.c	40.0	20.0	19.0	29135	0.1875	0.1875	2.0	0.1875	---	---	17.501	21.562	7.699	0.802	-6.1%
104.a	30.0	32.0	0.0	28589	0.1875	0.1875	2.0	0.1875	0.281	4.8%	15.156	18.673	6.718	1.244	-8.4%
104.c	30.0	32.0	31.0	28589	0.1875	0.1875	2.0	0.1875	---	---	15.156	18.673	6.718	1.244	-8.3%
105.a	40.0	32.0	0.0	41847	0.2188	0.1875	2.0	0.1875	0.231	1.2%	17.501	21.562	7.699	0.802	-6.4%
105.c	40.0	32.0	31.0	41847	0.2188	0.1875	2.0	0.1875	---	---	17.501	21.562	7.699	0.802	-6.1%
106.a	50.0	32.0	0.0	66569	0.2500	0.2500	2.0	0.2500	0.235	1.1%	22.594	24.107	10.668	0.711	-12.7%
106.c	50.0	32.0	31.0	66569	0.2500	0.2500	2.0	0.2500	---	---	22.594	24.107	10.668	0.711	-12.5%

Table A9-2: Results using simplified design calculations (1.0 inch slope)

Tank Data									Design Calculations						
Case	Dia (ft)	Height (ft)	Liquid Level (ft)	Weight (lb)	Bottom Course (in)	Top Course (in)	Angle Width (in)	Angle Thick (in)	First Uplift (psi)	First Uplift Error	Top Failure				
											wc (in)	wh (in)	A (in^2)	Ptop (psi)	Ptop Error
201.a	20.0	20.0	0.0	12111	0.1875	0.1875	2.0	0.1875	0.268	0.8%	8.632	10.446	3.952	3.293	-15.8%
201.c	20.0	20.0	19.0	12111	0.1875	0.1875	2.0	0.1875	---	---	8.632	10.446	3.952	3.293	-15.6%
202.a	30.0	20.0	0.0	20009	0.1875	0.1875	2.0	0.1875	0.197	0.7%	10.572	12.794	4.756	1.762	-14.8%
202.c	30.0	20.0	19.0	20009	0.1875	0.1875	2.0	0.1875	---	---	10.572	12.794	4.756	1.762	-14.8%
203.a	40.0	20.0	0.0	29135	0.1875	0.1875	2.0	0.1875	0.161	0.6%	12.208	14.773	5.434	1.132	-12.8%
203.c	40.0	20.0	19.0	29135	0.1875	0.1875	2.0	0.1875	---	---	12.208	14.773	5.434	1.132	-12.9%
204.a	30.0	32.0	0.0	28589	0.1875	0.1875	2.0	0.1875	0.281	4.8%	10.572	12.794	4.756	1.762	-14.8%
204.c	30.0	32.0	31.0	28589	0.1875	0.1875	2.0	0.1875	---	---	10.572	12.794	4.756	1.762	-14.8%
205.a	40.0	32.0	0.0	41847	0.2188	0.1875	2.0	0.1875	0.231	1.2%	12.208	14.773	5.434	1.132	-12.8%
205.c	40.0	32.0	31.0	41847	0.2188	0.1875	2.0	0.1875	---	---	12.208	14.773	5.434	1.132	-12.9%
206.a	50.0	32.0	0.0	66569	0.2500	0.2500	2.0	0.2500	0.235	1.1%	15.760	16.517	7.537	1.005	-19.2%
206.c	50.0	32.0	31.0	66569	0.2500	0.2500	2.0	0.2500	---	---	15.760	16.517	7.537	1.005	-19.3%

Table A9-3: Results using simplified design calculations (2.0 inch slope)

Tank Data									Design Calculations						
Case	Dia (ft)	Height (ft)	Liquid Level (ft)	Weight (lb)	Bottom Course (in)	Top Course (in)	Angle Width (in)	Angle Thick (in)	First Uplift (psi)	First Uplift Error	Top Failure				
											wc (in)	wh (in)	A (in^2)	Ptop (psi)	Ptop Error
301.a	20.0	20.0	0.0	12111	0.1875	0.1875	2.0	0.1875	0.268	0.8%	5.037	8.292	2.874	3.593	-0.7%
301.c	20.0	20.0	19.0	12111	0.1875	0.1875	2.0	0.1875	---	---	5.037	8.292	2.874	3.593	-0.5%
302.a	30.0	20.0	0.0	20009	0.1875	0.1875	2.0	0.1875	0.197	0.7%	6.169	10.155	3.436	1.909	0.3%
302.c	30.0	20.0	19.0	20009	0.1875	0.1875	2.0	0.1875	---	---	6.169	10.155	3.436	1.909	0.1%
303.a	40.0	20.0	0.0	29135	0.1875	0.1875	2.0	0.1875	0.161	0.6%	7.124	11.726	3.909	1.222	1.8%
303.c	40.0	20.0	19.0	29135	0.1875	0.1875	2.0	0.1875	---	---	7.124	11.726	3.909	1.222	1.6%
304.a	30.0	32.0	0.0	28589	0.1875	0.1875	2.0	0.1875	0.281	4.8%	6.169	10.155	3.436	1.909	0.3%
304.c	30.0	32.0	31.0	28589	0.1875	0.1875	2.0	0.1875	---	---	6.169	10.155	3.436	1.909	0.4%
305.a	40.0	32.0	0.0	41847	0.2188	0.1875	2.0	0.1875	0.231	1.2%	7.124	11.726	3.909	1.222	1.9%
305.c	40.0	32.0	31.0	41847	0.2188	0.1875	2.0	0.1875	---	---	7.124	11.726	3.909	1.222	1.8%
306.a	50.0	32.0	0.0	66569	0.2500	0.2500	2.0	0.2500	0.235	1.1%	9.197	13.110	5.257	1.051	0.0%
306.c	50.0	32.0	31.0	66569	0.2500	0.2500	2.0	0.2500	---	---	9.197	13.110	5.257	1.051	0.0%

Table A9-4: Results using simplified design calculations (3.0 inch slope)

API®

American Petroleum Institute

2005 Publications Order Form

Effective January 1, 2005.
API Members receive a 30% discount where applicable.
The member discount does not apply to purchases made for the purpose of resale or for incorporation into commercial products, training courses, workshops, or other commercial enterprises.

Available through Global Engineering Documents:
Phone Orders: **1-800-854-7179** (Toll-free in the U.S. and Canada)
303-397-7956 (Local and International)
Fax Orders: **303-397-2740**
Online Orders: **www.global.ihs.com**

Date: _____ ❑ **API Member** (Check if Yes)

Invoice To (❑ Check here if same as "Ship To")

Name:
Title:
Company:
Department:
Address:
City: State/Province:
Zip/Postal Code: Country:
Telephone:
Fax:
E-Mail:

Ship To (UPS will not deliver to a P.O. Box)

Name:
Title:
Company:
Department:
Address:
City: State/Province:
Zip/Postal Code: Country:
Telephone:
Fax:
E-Mail:

Quantity	Product Number	Title	SO★	Unit Price	Total
	C62010	Std 620, Design and Construction of Large, Welded, Low-pressure Storage Tanks		$242.00	
	C65010	Std 650, Welded Steel Tanks for Oil Storage		$289.00	
	C65102	RP 651, Cathodic Protection of Aboveground Storage Tanks		$78.00	
	C65202	RP 652, Lining of Aboveground Petroleum Storage Tank Bottoms		$78.00	
	C65303	Std 653, Tank Inspection, Repair, Alteration, and Reconstruction		$176.00	
	C93701	Publ 937, Evaluation of Design Criteria for Storage Tanks with Frangible Roof Joints		$118.00	
	C939D0	TR 939-D, Stress Corrosion Cracking of Carbon Steel in Fuel Grade Ethanol: Review and Survey		$63.00	
	C20005	Std 2000, Venting Atmospheric and Low-pressure Storage Tanks: Nonrefrigerated and Refrigerated		$98.00	

❑ **Payment Enclosed** ❑ **P.O. No.** (Enclose Copy) _____

❑ **Charge My Global Account No.** _____

❑ **VISA** ❑ **MasterCard** ❑ **American Express** ❑ **Diners Club** ❑ **Discover**

Credit Card No.:
Print Name (As It Appears on Card):
Expiration Date:
Signature:

Subtotal	
Applicable Sales Tax *(see below)*	
Rush Shipping Fee *(see below)*	
Shipping and Handling *(see below)*	
Total *(in U.S. Dollars)*	

★ ***To be placed on Standing Order for future editions of this publication, place a check mark in the SO column and sign here:***

Pricing and availability subject to change without notice.

Mail Orders – Payment by check or money order in U.S. dollars is required except for established accounts. State and local taxes, $10 processing fee*, and 5% shipping must be added. Send mail orders to: **API Publications, Global Engineering Documents, 15 Inverness Way East, M/S C303B, Englewood, CO 80112-5776, USA.**
Purchase Orders – Purchase orders are accepted from established accounts. Invoice will include actual freight cost, a $10 processing fee*, plus state and local taxes.
Telephone Orders – If ordering by telephone, a $10 processing fee* and actual freight costs will be added to the order.
Sales Tax – All U.S. purchases must include applicable state and local sales tax. Customers claiming tax-exempt status must provide Global with a copy of their exemption certificate.
Shipping (U.S. Orders) – Orders shipped within the U.S. are sent via traceable means. Most orders are shipped the same day. Subscription updates are sent by First-Class Mail. Other options, including next-day service, air service, and fax transmission are available at additional cost. Call 1-800-854-7179 for more information.
Shipping (International Orders) – Standard international shipping is by air express courier service. Subscription updates are sent by World Mail. Normal delivery is 3-4 days from shipping date.
Rush Shipping Fee – Next Day Delivery orders charge is $20 in addition to the carrier charges. Next Day Delivery orders must be placed by 2:00 p.m. MST to ensure overnight delivery.
Returns – All returns must be pre-approved by calling Global's Customer Service Department at 1-800-624-3974 for information and assistance. There may be a 15% restocking fee. Special order items, electronic documents, and age-dated materials are non-returnable.
***Minimum Order –** There is a $50 minimum for all orders containing hardcopy documents. The $50 minimum applies to the order subtotal including the $10 processing fee, excluding any applicable taxes and freight charges. If the total cost of the documents on the order plus the $10 processing fee is less than $50, the processing fee will be increased to bring the order amount up to the $50 minimum. This processing fee will be applied before any applicable deposit account, quantity or member discounts have been applied. There is no minimum for orders containing only electronically delivered documents.

There's more where this came from.

The American Petroleum Institute provides additional resources and programs to the oil and natural gas industry which are based on API® Standards. For more information, contact:

• API Monogram® Licensing Program	Phone:	202-962-4791
	Fax:	202-682-8070
• American Petroleum Institute Quality Registrar (APIQR®)	Phone:	202-962-4791
	Fax:	202-682-8070
• API Spec Q1® Registration	Phone:	202-962-4791
	Fax:	202-682-8070
• API Perforator Design Registration	Phone:	202-962-4791
	Fax:	202-682-8070
• API ISO/TS 29001 Registration	Phone:	202-962-4791
	Fax:	202-682-8070
• API Training Provider Certification Program	Phone:	202-682-8490
	Fax:	202-682-8070
• Individual Certification Programs	Phone:	202-682-8064
	Fax:	202-682-8348
• Engine Oil Licensing and Certification System (EOLCS)	Phone:	202-682-8516
	Fax:	202-962-4739
• API PetroTEAM™ (Training, Education and Meetings)	Phone:	202-682-8195
	Fax:	202-682-8222

Check out the API Publications, Programs, and Services Catalog online at www.api.org.

API
American Petroleum Institute

Helping You Get
The Job Done Right.®

Additional copies are available through Global Engineering Documents at (800) 854-7179 or (303) 397-7956

Information about API Publications, Programs and Services is available on the World Wide Web at http://www.api.org

American Petroleum Institute

1220 L Street, Northwest
Washington, D.C. 20005-4070
202-682-8000

Product No: C937A0